Role of connexin36 proteins in peripheral nerves during the triple response and pain

by

Prabhpal Kaur Bhullar

A Thesis submitted to the Faculty of Graduate Studies of

The University of Manitoba

In partial fulfilment of the requirements of the degree of

MASTER OF SCIENCE

Department of Physiology and Pathophysiology

University of Manitoba

Winnipeg

Abstract

Introduction: Gap junctions allow direct cell-to-cell communication and form electrical synapses between neurons primarily via the gap junction protein connexin36 (Cx36). We examined the potential contribution of Cx36 in spinal dorsal root ganglia and peripheral nerves to the classic triple response (flare, wheal, and edema) following stimulation of nociceptors. The flare reflects increased blood flow beyond the injured area and the wheal is due to changes in the vascular permeability. Studies conducted in the 1980s suggested that electrical coupling between unmyelinated C-fibers in the periphery may contribute to these responses. Cx36 is a protein allowing gap junction formation between neurons.

Objectives: We aimed to quantify the contribution of Cx36-containing gap junctions to plasma extravasation responses following stimulation of nociceptors.

Methods: Wild-type (WT) and Cx36 knockout (KO) mice lacking this protein in all neurons were used for studies in which application of noxious stimuli (xylene, formalin, electrical stimulation of the sciatic nerve) was performed. Extravasation of Evans Blue dye from the circulation in the limbs was monitored via spectrophotometry, laser Doppler flux and *in vivo* fluorescence imaging after noxious stimulation in anesthetized mice.

Results: A small but non-significant difference was found between KO and WT animals in the extravasated EB dye after front-paw's chemical stimulation with xylene. A trend for greater responses as well as a faster rate of change in the Evans Blue fluorescence was found within the first 2-5 minutes after xylene application in WT vs. KO mice.

Conclusions: The enhanced early vascular response observed in this study after nociceptor stimulation in the WT animals as compared to the KO animals is consistent with earlier reports

of direct electrical coupling between C-fibers and with evidence of Cx36 expression in small sensory neurons. These results suggest that Cx36 transiently contributes to the triple response.

Acknowledgements

I wish to acknowledge all those persons who have left a mark on this work through their encouragement, support, comments and criticism.

I would first like to thank my thesis advisor Dr. Katinka Stecina for guiding me at every step of the way. Her mentorship has been an invaluable gift for my graduate life. My research work, writings, queries were always provided with productive feedback by her. I would also like to express my sincere gratitude to my co-supervisor and committee member, Dr. James I. Nagy for steering this work in right directions. I am extremely grateful to him for sharing his immense knowledge with me. I am also thankful to Dr. Michael F. Jackson, my committee member for his insightful comments and hard questions. I appreciate the input provided by my committee members at every stage of this research project.

My deepest appreciation goes to Dr. Mike Jackson and Dr. Bruce Lynn for sharing their knowledge and expertise with me in the field of *in vivo* imaging and spectrophotometry. Special thanks to Sharon McCartney and Maria Setterbom for all the instances in which their assistance helped me along the way. I would also like to thank Matt Ellis and Gilles Detillieux for all of their computer and technical assistance throughout my graduate program. I must also acknowledge the young bright mind, Shu ting Zhao, co-op student, for her contribution to this work.

In conclusion, I also want to recognize the financial support provided by NSERC and Research Manitoba for this research project and express my gratitude to those agencies.

Contents

List of Tables

List of Figures

List of Key Abbreviations

CFP	Control Front Paw
CHP	Control Hind Paw
CGRP	Calcitonin gene-related peptide
CNS	Central Nervous System
Cx36	Connexin36 protein
DRG	Dorsal Root Ganglia
EB	Evans blue
EV	extravasation
KO	Knockout
ROI	Region of interest
SFP	Stimulated Front Paw
SHP	Stimulated Hind Paw
SP	Substance P
TFC	Total fluorescent voxel counts
WT	Wildtype

1. Introduction

1.1. Connexin proteins and Cx36

Connexins are integral transmembrane proteins that assemble to form channels between the membranes of two neighboring cells (Dermietzel & Spray, 2013). The connexin family of proteins has 21 homologs in humans and 20 in mice (Dermietzel & Spray, 2013). They are named with acronym **Cx** (i.e. connexin) followed by their molecular mass in kDa. Each connexin is formed of four transmembrane domains with cytoplasmic amino and carboxyl tails. The transmembrane domains are connected via one intracellular loop and two conserved extracellular loops that have three cysteine residues each (Evans & Martin, 2002). Connexins from one cell form a connexon. A connexon is a hexameric unit that is also called a hemichannel. A single gap junction is composed of two connexons contributed by each of the neighboring cells (Dermietzel & Spray, 2013). One cell has generally more than on type of connexin protein. The hexameric units can be homomeric - formed of one type of connexin isoform or they can be heteromeric - formed by at least two types of connexin proteins. This leads to different configurations of gap junction channels - formed by the same connexin type in each apposing connexon and heterotypic being different connexin types in each apposing connexon (Dermietzel & Spray, 2013).

The connexin isoforms found in vertebrate neurons are connexin36 (**Cx36**), Cx45, Cx50, Cx30.2 and Cx31.1 (Pereda, 2014). Cx36 is considered the major neuronal connexin (Pereda, 2014) allowing two neighboring neurons to connect. In early developmental stages, Cx36 is broadly expressed in the brain. Its expression falls after the second week of embryonic development and Cx36 expression becomes confined to neurons only (Hartfield et al., 2011). Cx36 is abundantly expressed in the neurons of the retina, dentate gyrus, hippocampus, cerebral

and piriform cortexes, amygdala, cerebellum, mesencephalon, suprachiasmatic nucleus, thalamus, hypothalamus, and various brain stem nuclei (Dere & Zlomuzica, 2012). Cx36 is also found in lumbar motoneurons of neonatal rats (Bautista et al., 2014).

1.2. Gap junctions

Gap junctions are a direct way of connecting the cytoplasm of two neighboring cells. Cx36 allows such direct connection between the cytoplasm of two neighboring neurons. Gap junctions can be present between dendrites, between somata, or between dendrites and somata in the mammalian central nervous system (Nagy et al., 2013). Gap junctions can also be present in glial cells of the **CNS**. Astrocytes are extensively coupled by gap junctions formed of Cx43 and Cx30. Oligodendrocytes expresses mainly Cx32 and Cx47 (Dere & Zlomuzica, 2012).

Electrical transmission via gap junctions differs from chemical transmission in several aspects such as directionality, speed and excitability (Dermietzel & Spray, 2013). Electrical synapses lack the complex presynaptic and postsynaptic membranes found in chemical synapses. Instead they allow direct cell-to-cell communication of electrical signals and small molecules (approx. 1kDa in size) such as calcium, cyclic AMP and inositol-1,4,5-trisphosphate (Pereda, 2014). This signal transmission is mostly bidirectional whereas chemical synapses provide transmission in one direction (Dermietzel & Spray, 2013). Moreover, electrical synapses have faster transmission speed than chemical synapses. Chemical transmission can be excitatory or inhibitory depending on the neurotransmitter that is released in the synaptic cleft. Electrical synapses, on the other hand, are mostly excitatory thereby often leading to synchronous firing of cells (Dermietzel & Spray, 2013).

The evidence of electrical transmission between neurons emerged in 1950's from work done on giant motor synapses of the crayfish (Furshpan & Potter, 1959) and on neurons of the cardiac

ganglion in the lobster (Watanabe, 1958). Morphological evidence for the presence of neuronal gap junction channels was first found in goldfish at the Mauthner cell synapses (Robertson et al., 1963). Gap junctions allow synchrony within networks by allowing metabolic as well as electrotonic coupling of neighboring cells (Evans & Martin, 2002). Some of the best examples for gap junctions that mediate synchrony are in cilia of tracheal epithelial cells. These cilia beat rhythmically to clear mucus from the trachea. Another example is cardiac myocytes enabling rhythmic pumping of the heart (Evans & Martin, 2002). Whole cell recording techniques have been used to confirm that sympathetic preganglionic neurons in rat exhibit gap junction-mediated coupling (Logan et al.,1996) and that electronic coupling is present in cat motoneurons (Gogan et al., 1977).

1.3. Dorsal root ganglia; neurogenic inflammation; vasodilation and extravasation

Cx36 has been found in the superficial dorsal horn of neonatal and the adult mammalian spinal cord, suggesting a role in sensory function (Lemieux et al., 2010). Cx36 puncta found in the adult mouse spinal cord have a regulatory role in presynaptic inhibition involving large diameter sensory fibers and spinal presynaptic inhibitory interneurons (Bautista et al., 2012). Cx36 is also expressed in axon terminals of primary afferent neurons in adult rat spinal cord where they form mixed synapses (Bautista et al., 2014).

Dorsal root ganglia (**DRG**) are groups of neuronal somata of primary afferent - or sensory-neurons. They are pseudo unipolar cells as they have an axon that gives off two branches: one branch extending from the DRG to the spinal cord and the other one projecting from the DRG to the periphery. Peripheral nerve endings of the DRG terminate as free nerve endings or they are associated with special sensory receptors in the tissue they innervate (Holzer, 1988). Primary afferent neurons are generally thought to have sensory functions because DRG axons carry

signals from various receptors to the central nervous system to activate effector systems. However, sensory nerve endings can also exert local effector function as, for example, during the inflammatory responses after injury (Holzer, 1988).

Sensory neurons were first described to have local effector function when peripheral processes of these neurons were cut centrally and the nerves were stimulated. The stimulation induced vasodilation in the periphery and this response was found to be independent of autonomic nervous system output (Bayliss, 1901). The stimulation which induced this vasodilation resulted from action potentials conducted from the proximal region (with respect to the spinal cord) to the periphery along the axons of DRG which is in the opposite direction than the normally occurring way in these neurons. Therefore, the vasodilation induced by the stimulation of a nerve that is cut centrally has been termed as antidromic vasodilation. Antidromic vasodilation has been also recognized as a component of the inflammatory process following the application of chemical irritants such as mustard oil. As suggested by the lack of vasodilation in skin and conjunctiva when sensory denervation has been applied, peripheral sensory endings have been deemed crucial for this process to manifest after stimulation of nociceptors (Bruce, 1913). Nociceptors are sensory neurons that transmit pain sensation. In other words, these are specialized receptors that respond to the stimuli that would be damaging to live tissue; such as high temperature or pressure or chemical irritants (Dubin & Patapoutian, 2010). Because of the crucial role of sensory neurons in antidromic vasodilation, this process came to be known as neurogenic inflammation. The common definition of neurogenic inflammation is: inflammation arising from the local release of inflammatory mediators by afferent neurons (Lynn et al., 1988; Melzack & Wall, 1999). In addition to vasodilation, the antidromic stimulation of sensory nerves also results in increased vascular permeability. The increased permeability leads

to more blood plasma escaping from the blood vessels after stimulation. The escape of the blood plasma from vessels to the surrounding tissue is also called as extravasation (**EV**).

1.4. The inflammatory triple response, the axon reflex and coupling between nerve fibers

After an injury to the skin, the responses of the blood vessels are three fold; hence it bears the name triple response (a.k.a. the response of Lewis) (Lewis, 1927; Lewis & Zotterman, 1927). Firstly, there is local reddening of the injured area (or flush) that is followed by the redness extending to non-injured skin regions. This second process is called flare. Following the flare, there is wheal formation. In other words, there is first a local vasodilation in the injured area, then this vasodilation spreads to the neighboring blood vessels and the response is topped by increased vascular permeability leading to plasma extravasation i.e. how the wheal is formed.

These inflammatory responses were found to be inhibited by desensitization of nerve fibers after capsaicin application (Jancso et al., 1967) and the sensory fibers responsible for them were concluded to be the small diameter, unmyelinated, C-fibers (Hinsey & Gasser, 1930). Lewis stated originally, that an inflammatory mediator may also be involved which helps in facilitating vasodilation and that is similar to histamine (Lewis, 1927). This neurohumor- referring to an inflammatory mediator having a vital role in facilitating inflammatory responses - was later identified to include various neuropeptides present in primary afferent neurons that are released at the periphery upon injury. Commonly known inflammatory mediators include Substance P (SP), calcitonin gene-related peptide (**CGRP**), neurokinin A (NKA), and endothelin-3 (ET-3) (Holzer, 1998).

Substance P (**SP**) was the first potential mediator to be identified (Holton, 1959; Lembeck, 1953). It was found in unmyelinated C fibers innervating the skin. It is released at the terminals of sensory neurons on antidromic stimulation (Cuello et al., 1976; Hökfelt et al., 1977). When SP

is secreted, it binds to the tachykinin receptors NK1 on endothelium cells of blood vessel. This NK1 receptor binding by SP results in vasodilation and plasma protein leakage. SP can also act on mast cells and leucocytes that become activated by SP and they release inflammatory molecules such as cytokines, prostaglandins and histamine (Holzer, 1998). Other neuropeptides such as CGRP, neurokinin A (NKA) and neurokinin B (NKB) (Holzer, 1998) act on different receptors. CGRP acts on CGRP1 receptors present on endothelium of arterioles and it can also induce vasodilation. However, it does not play an active role in causing plasma EV (Holzer, 1998).

In addition to the release of inflammatory mediators, another physiological mechanism, called the axon reflex, is also likely to contribute to the triple response (Lewis, 1927). The axon reflex term was first used in the context of the pilomotor reflex induced upon stimulation of the sympathetic chain as the proposed mechanism behind the responses in the pre-ganglionic fibers (Langley, 1900). In the context of neurogenic inflammation, the idea of the axon reflex was first used by Bruce (1913), who proposed the axon reflex is the mechanism behind antidromic vasodilation. Based on his proposal, the axon reflex was later considered to be contributing also to the classic triple response (Lewis, 1927).

The axon reflex explains that sensory fibers at the periphery branch out with some of the branches innervating the blood vessel and other branches innervating the skin (as free nerve endings). When cutaneous sensory receptors are activated, nerve impulses are generated that travel centrally along the main axon of the DRG. The action potentials, however, also travel in the opposite direction, antidromically, and thereby possibly transmitted in branches that innervate blood vessel. The antidromically transmitted action potentials, therefore, could induce

vasodilation in the innervated vessels resulting in flush beyond the injured skin area (Lewis, 1927; Yaprak, 2008).

In addition to the antidromic spread of action potentials in sensory endings following nociceptor activation, the nerve endings adjacent to injured skin may also be activated by coupling of the fibers. Investigations done in monkeys revealed that unmyelinated fibers of the peripheral nerve exhibit bidirectional electrical coupling near the receptor endings (Meyer et al., 1985). This electrical coupling could facilitate the spread of action potentials to neighboring fibers (Meyer et al., 1985).

If electrical coupling is present in the axons of DRG neurons, then gap junctions may be involved in connecting the neighboring axons at the periphery. These gap junctions occur between two neurons, thus they may be formed by Cx36 proteins. In a recent immunofluorescence study investigating the expression of Cx36 in the laboratory of Dr. J. Nagy, Cx36 was examined by the use of a reporter protein (EGFP) in DRG of a genetically modified line of mice along with other markers such as SP and CGRP (Zhao et al., 2015). This preliminary study has found that half of the SP positive neurons and a quarter of CGRP positive neurons also contained EGFP reporter for Cx36.

These results lead to the hypothesis that the presence of Cx36 protein results in enhanced responses to nociceptor activation. As depicted in Fig. 1.1., Cx36 is present in the DRG neurons and functional gap junctions at the periphery, near the receptor endings of the afferents, allowing direct coupling between nerve fibers. During the triple response, Cx36 containing gap junctions facilitate communication between nociceptors and help in spreading nerve impulses to neighboring fibers. We hypothesize that the presence of Cx36 leads to increased vasodilation and

vascular permeability and to flare occurring at a greater extent and/or at a faster rate than it would occur in the absence of Cx36.

Figure 1.1. here

1.5. Research aims

In order to test the above hypothesis, I have conducted studies to assess differences in vasodilation and plasma extravasation responses in two different strains of mice. I have utilized a genetically modified strain of animals from the Nagy laboratory. These animals lack the Cx36 protein due to a knock-out mutation (**KO**) originally developed from C57/BL6-129SvEv mixed background (Deans et al., 2001). The other line was a normal, wild-type (**WT**) mouse line with the same genetic background as the KO strain, from a colony on site that was established from breeding pairs generously donated by Dr. D. Paul (Harvard) to Dr. J. Nagy. Comparisons of the vasodilation and plasma extravasation were made between the responses of KO and WT mice following nociceptor activation.

In order to quantify the extent of vasodilation and plasma extravasation in response to nociceptor activation, several methods have been used in pain research. One of the oldest techniques relies on Evans blue dye (**EB**), a tracer used for estimation of plasma volume and extravasation (Drygalski et al., 2012; Jancso et al., 1967; Szolcsányi, 1988; Wang & Lai, 2014). The EB dye binds to albumin rapidly after intravenous injection but it is non-toxic, non-metabolically active and it does not undergo cellular uptake. The EB concentration can be used to estimate total plasma volume in the injected test subjects shortly after its administration and it can be also used to correlate vascular leakage of serum albumin by measuring its concentration in central and peripheral organs (Wang & Lai, 2014). The final extravasated concentration of EB can be quantified by light spectrometry. This requires that the vessels are cleared and the skin or

the organ is removed after the nociceptor stimulation phase has ended. Then the EB is isolated before light spectral readings are performed on the tissue extracts. The EB quantity thus represents terminal (end) responses in terms of the vascular leakage attributable to the nociceptor activation. The first aim of my study was to test whether the EB extracted from the paws after nociceptor stimulation is different between the KO and WT animals.

As Cx36 is more likely to influence the very early responses after nociceptor activation, another method that is more suited for detecting immediate or early responses was also utilized here. Laser Doppler-based flow-metry represents another classic method that has been used to monitor blood flow and microcirculatory changes in live tissue. The premise behind using this method is that emitting monochromatic light through the mouse skin will reflect off of red blood cells in the vasculature, resulting in a change of frequency in the reflected light upon changes in blood volume or flow (Choi & Bennett, 2003). There is also a second portion of light that is not scattered which is the "transmitted" light. Together, these two portions of light at different frequencies result in phenomena called beat frequency which is recorded by the probe and the monitor. These beat frequencies are analyzed and they are used to create an indirect measure of red blood cell velocity (Choi & Bennett, 2003). The unit of measurement used to quantify the velocity of red blood cell movement is an arbitrary unit called "flux" derived from a number of different formulations (Choi & Bennett, 2003). Flux is defined as the product of the movement of red blood cells in a given volume and the mean net velocity of its movement (Choi & Bennett, 2003). The main difference between using EB dye intravenously injected and then extracted from the skin versus recording the flux changes is that the former is strictly a measure of the extravasation (not confounded by blood flow changes) while the latter is a composite of changes not only in the escaped dye (or plasma) but also the volume changes within the vessels. The

second aim of my study was to test whether the immediate changes to nociceptor stimulation were different between the KO and WT animals.

In addition to the above mentioned validated methods of EB quantification, I have also employed a third, novel method here. This third method was *in vivo* small animal fluorescence imaging because EB is a fluorescent dye. The utility of this novel technique has been its high sensitivity for lower amounts of EB injected into the circulation. This technique also allowed the real time comparison of the baseline EB levels prior to stimulation within the peripheral organs of interest (in this study, the hind paws).

1.6. Experimental models used for nociceptor stimulation

There are several chemical irritants that are known to cause neurogenic inflammation such as capsaicin, mustard oil, xylene and formalin. Capsaicin-induced inflammation is widely studied and it involves activation of the transient receptor potential vanilloid type 1 receptor ion channel (TRPV1) on primary sensory neurons. These ion channels are critical mediators of nociception as learned from experiments on mice lacking this receptor which do not show pain related behavior (Caterina et al., 2000). However, when capsaicin is applied in higher concentrations, it can result in functional block of the TRPV1 nociceptors.

Xylene, an industrial and commercial solvent, is a skin irritant and a sensitizing agent (Sándor et al., 2009) that has been used to induce neurogenic inflammation (Jancso et al., 1967). When topically applied, it activates sensory nerves and causes inflammation. Different concentrations of xylene (10-100%) are known to result in concentration dependent increases in vascular permeability and xylene induced plasma extravasation was categorized into early and late responses (Maggi et al., 1988). Xylene also involves TRPV1 receptor stimulation. In

knockout mice lacking TRPV1 channels, no nociceptive behavior such as paw liftings and shakings was seen on xylene exposure (Sándor et al., 2009).

Formalin or formaldehyde is an important precursor to many other materials and chemical compounds (its synthetic name is methanal). It is mainly used in the production of industrial resins, such as particle board and coatings ("Formaldehyde," n.d.). Formalin test in pain research was first standardized in rat and cats by Dubuisson and Dennis in 1977 (Dubuisson & Dennis, 1977). The response to formalin (0.1 ml of 5%) was categorized into two phases: short lasting (early) phase and a later phase. The early response has been reasoned to be caused by direct effect of formalin on sensory receptors and it lasts for few minutes. The later response has been reasoned to be due to inflammation (lasting for about 45-60 minutes) after the nociceptive stimulation has been initiated (Clavelou et al., 1989; Miampamba et al., 1994; Roveroni et al., 2001). In this original study using formalin, it was injected into the forepaw and the resulting tonic pain was evaluated according to objective behavioral criteria (Dubuisson & Dennis, 1977). The commonly used procedures when using formalin for pain studies are that it is injected subdermally or systemically in concentration from 0.5-5%.

2. Methods

2.1. Declaration of ethics compliance

Prior to the commencement of this work, all experimental protocols have been approved by the Animal Care Committee of the Office of Research Ethics and Compliance at the University of Manitoba; in accordance with the regulations set by the Canadian Council on Animal Care. Animals from two different strains of mice: B6;129S4 Gjd2tm 1 (the KO mice) and B6;129S4 Gjd2 Wt (the WT mice) were used. Overall, 48 mice (18-45 g) have been used for these studies. There were two main series of experiments conducted:

1. *In vivo* mouse electrophysiology experiments (12 animals).
2. *In vivo* mouse imaging experiments (38 animals).

The stimuli used to activate nociceptors in the above stated experiments were: xylene (100% or 75% diluted in mineral oil), 5% formalin (diluted in 0.9% saline) and electrical stimulation of the sciatic nerve after cutting it so action potentials could only be transmitted to the periphery.

2.2. *In vivo* mouse electrophysiology preparation surgery and procedures

Figure 2.1 illustrates the schematic of the mouse preparation used for the *in vivo* electrophysiology experiments. The mice were anesthetized with isoflurane, weighed and transferred to a heating pad and a nose-cone for maintained anesthesia. Vitals such as temperature were monitored using a rectal probe with feedback to the heat pad (TC-1000 Temperature controller, CWE, Inc.); a pulse oximetric monitor (Kent Scientific Corp. PhysioSuite) was used for tracking vital signs such as heart rate, temperature, breaths/minute, oxygen saturation. Saline was given every 30 minutes via an intraperitoneal (i.p.) catheter. Tracheotomy was performed and the animal was transferred to the ventilator (SAR-830/P Ventilator, CWE) to monitor end-tidal $C0_2$ levels (microCapStar CO2 Analyzer, CWE Inc. USA).

Figure 2.1. here

The sciatic nerve of the left hind limb was exposed and dissected free (Fig. 2.1). It was covered with a saline-soaked swab to prevent tissue drying. Laminectomy was performed between the 13^{th} thoracic (T13) and first lumbar (L1) vertebrae and the spinal cord was exposed. A “pool” was created around the exposed sciatic nerve by using the skin flaps of the exposed area and by securing them to the recording frame with threads. This “pool” was filled with mineral oil to prevent tissue drying.

The laser Doppler blood flow monitor (Moor Instruments floLAB/moorLAB, UK) was used to measure the microcirculatory changes (flux recording as shown in the insert in Fig. 2.1) distal to the sciatic nerve stimulation site in half of the animals used for *in vivo* electrophysiology. This probe was placed below the 5th digit on the left hind paw over a small, 1mm diameter circular region after calibrating it with a standard solution (PFS flux standard, Moor Instruments, UK).

Silver electrodes were placed on the spinal cord (ball electrode) and on the sciatic nerve (hook electrode). The electrode on the surface of the spinal cord near the T13-L1 border was used to measure the so called cord dorsum potentials (CDPs). These CDPs reflect incoming action potentials from the stimulated peripheral nerve fibers as well as the action potentials of spinal neurons near the electrode (Willis, 1980) based on the latency of the different components. The CDPs were used in each animal to scale the stimulus intensity in terms of the strength required for the activation of the most excitable (largest diameter) afferents. This intensity, called the threshold, or T, was increased up to 100 times as the type of recruited afferents can be scaled by using this method (Jack, 1978). The small diameter myelinated afferents are maximally recruited at about 5-10X T, while the unmyelinated afferents are recruited at a range between 30 – 100xT (Jack, 1978; Li & Bak, 1976). Once the T voltage was established for the sciatic nerve, this nerve was cut to prevent autonomic and other centrally initiated responses following nociceptor activation. In order to prevent muscle twitching during the electrical stimulation, pancuroniumm bromide was given to the animal prior to commencing all electrical stimulation (0.1 mg/kg, i.p.).

The animal was given a retro-orbital injection of Evans blue dye (50 mg/kg) from a stock with concentration of 50 mg/mL (Yardeni et al., 2011). Once the dye dispersion in the circulation

was visually verified (i.e. the skin and the cut tissue showing blue discoloration) xylene (100%, 20uL) was placed on one of the front paw with an Eppendorf pipette. Subsequently, the electrical stimulation of the cut sciatic nerve commenced and different intensities were tested while recording the flux changes. Different intensities were tested in different bouts, while using 0.2 ms square pulses at 3, 5 and 20 Hz as suggested by previous studies on rats (Carmichael et al., 2008).

After electrical nerve stimulation trials, the animal was transcardially perfused with 100 ml of phosphate buffer solution (30 ml 0.5 phosphate buffer solution, 10 ml 0.9% saline, 60 ml of distilled water). The skin tissue was removed from the hind and front paws. This "wet tissue" was weighed and placed into 500 µl of formamide solution for incubation in a warm bath (at 56-60 ^{0}C for 21-24 hours). Then the samples were transferred to a -80 ^{0}C freezer until spectrometric analysis was done on the samples.

2.3. *In vivo* small animal fluorescence imaging procedures

In vivo imaging was performed using a Perkin Elmer/Caliper IVIS Spectrum optical imaging system which used epi-illumination. Fluorescence imaging was done by using a CCD camera which was cooled to -90 ^{0}C before beginning the acquisition.

The animal was anesthetized in an induction chamber with isofluorane, it was weighed, and then transferred to a nose cone for maintained anesthesia. After establishing the absence of pedal reflexes, 10 µl Evans blue dye from a stock solution of 50 mg/ml was retro-orbitally injected. The animal was transferred to a nose cone in the imaging chamber immediately and within 30 s after the Evans blue dye injection the acquisition of the fluorescent images was initiated. Imaging with exposure times of 10 sec, with excitation and emission filters at 605 nm

and 700 nm, respectively was done throughout each experiment. The imaging in the first 5 minutes was used to establish a baseline as shown in Fig. 2.2A.

Then one hind paw of was chemically stimulated by the topical application of xylene (15 µl, concentration 100%, 75%) or by the intradermal injection of formalin (5%, 0.02-0.03 ml with a 26G needle). After starting the stimulation, the chamber door was closed and images were acquired again with parameters as during the baseline period for 15 to 30 minutes. In case of xylene, usually 15 min and in case of formalin, up to 20-30 minutes of imaging was done as illustrated in Fig. 2.2B. After data acquisition, the animal was removed from the chamber and euthanized by cervical dislocation and bilateral pneumothorax.

Figure 2.2. here

2.4. Analysis of Evans blue extravasation

The light spectrometry was done by first centrifuging the tubes containing the skin and formamide and the supernatant was separated by manual pipetting. Then 100 µl of each supernatant sample was placed in a well as shown in Fig. 2.3.B. Standard dilutions of Evans blue dissolved in formamide were also prepared for analysis (square in Fig. 2.3.B) together with the obtained samples. A standard curve as shown in Fig. 2.3.C was acquired from the measurements of the wells with the serial dilutions and this curve was used to derive an equation for calculating the amount of dye in the samples. The obtained values were normalized to the wet tissue (expressed as microgram per milligram wet tissue, µg/mg).

Figure 2.3 here

The extracted dye measurements obtained from each paw were further normalized by taking the stimulation time into account i.e. dividing the µg/mg wet tissue numbers by the minutes of stimulation in each animal. Paired t-test (assuming one-tailed distribution, using t-test

function in Microsoft Excel) was used to compare the differences in the extracted dye between WT and KO animals. The standard errors of the means (SEM) were calculated by first computing the standard deviation and dividing that by the square root of the number of samples (also using Microsoft Excel).

2.5. Analysis of laser Doppler flux changes

The flux measurements obtained from the laser Doppler probe (as exemplified by the insert in Fig. 2.1) were quantified by deriving the flux amplitude changes and the area under the curve changes after stimulation with respect to baseline. The baseline levels were readings at one minute prior to each stimulation episode. The area and the amplitude were measured for the same duration during the baseline and the stimulated bouts and they gave similar results in terms of relative changes to baseline. Only the amplitude changes were used for illustrations here. Initially, data from age-matched WT and Cx36 KO mice were to be compared, but post-hoc these comparisons could not be performed as data without confounding variables were obtained from only three KO animals (see more in 3.2).

2.6. Analysis of *in vivo* fluorescence imaging data

The images were analyzed using the Living image software. On each hind paw, a specific region of interests (**ROI**) was selected from the photographs overlaid on the fluorescent images as shown in Fig.2.2.A-B. The dimensions of both ROIs were kept the same for each paw. The signal intensities (expressed as counts of fluorescent voxels) were obtained for each ROI. Both, the total counts of fluorescent voxels (**TFC**) in the ROIs and also the counts of fluorescent voxels with the maximum intensity within the ROIs were used initially for further analysis. The ratio of the counts in the ROIs of the stimulated paw vs. the non-stimulated paw (stimulated paw ROI / non-stimulated paw ROI) was calculated in each animal. The TFC was normalized at each

time point to the maximum value found within 15 minutes of stimulant application in each paw of each animal. Then the TFCs during the last 2 minutes (of the 5 minute long) baseline periods were averaged in order to create a baseline value in each paw of each animal. This baseline value was subtracted from the TFC values at each time point in order to account for baseline fluctuations. The rate of change in the TFCs was calculated by subtracting subsequent measurements in each paw that were collected exactly 30 s apart from each other. The difference obtained at each time point was again normalized to the maximal change occurring within 15 minutes of stimulant application in each paw of each animal.

Paired t-test (assuming one-tailed distribution) was used to test for significant differences at each time point between measurements (TFC or rate of change) obtained from WT and KO mice.

3. Results

In order to examine the contribution of Cx36 to peripheral responses after activation of nociceptors in the skin, two main series of experiments were performed. One series consisted of *in vivo* electrophysiology studies in adult, aged-matched KO and WT mice (n=12 animals). In this series, two types of stimuli (in the same animal, at the same time) were used to activate nociceptors: electrical stimulation of the cut sciatic nerve in one hind limb (always the left paw) and topical application of xylene in one forelimb (randomly selected left or right). Table 1 below provides details about each experiment in this series.

Table 1 here

The other series consisted of *in vivo* adult mouse fluorescence imaging on aged matched KO and WT mice (n=30 animals) and 8 additional non-age matched animals. In this series, one hind paw of each animal was subjected to one type of chemical stimuli that induced nociceptor

activation. Xylene and formalin was used in this series. Topical xylene application was tested at different strengths (100% in 9 pairs, 75% in 3 pairs and) and 5% formalin solution was injected intradermal in the paw (in 3 pairs). The additional trials for testing procedures, solvents and saline as negative controls were done with 8 animals: 6 KO and 2 WT. Knockouts were used to test saline and different dilutions of xylene (75% xylene diluted in ethanol (2 KO) and mineral oil (1 KO)) as the irritant. Two of these KO were the test trials for 5% formalin injection. The test trial with one wild-type animal used 50% xylene diluted in mineral oil. Trials were also done after electrical stimulation of sciatic nerve (one WT and one KO). None of these additional trials were used for comparative analysis and the results from these are not reported here. Table 2 below provides the key characteristics of each experiment in this series.

Table 2 here

3.1. Differences in blood plasma escape as measured by light spectral analysis

As illustrated in Figure 3.1A, extravasated Evans blue dye quantification from the skin covering each paw in the hind limb and the forelimb resulted in variable amounts (data from 10/12 animals as 2 mice died before the end of all required stimulation procedures likely as a results of over-anesthesia). The results showed great variations in the absolute amount of the escaped dye in both WT and KO mice i.e. note large error bars. The xylene stimulation of the front paws led to more extravasated dye in stimulated front paw than in the control forepaw (dotted line in Fig 3.2A) in WT animals, whereas in KO animals there was no difference between stimulated and control paws. However, there was no significant difference between the amount of dye between the WT and the KO mice in any of the four paws ($p=0.49$, 0.34, 0.11 and 0.29, for SFP, CFP, SHP and CHP respectively). The difference between chemically stimulated WT and KO front paws ($n=3$) was insignificant ($p=0.892$) as well as those between electrically

stimulated WT and KO hind paws (n=4) (p=0.05). The power of these t-test, however, was low (0.05 and 0.06 respectively) due to the large variation.

The duration of the chemical and the electrical stimulation was different in almost all of the tested animals (see Table 1). In order to account for these differences, the measured dye was normalized to the time of stimulation and the results are respectively illustrated in Fig.3.1.B and C for the age matched pairs (n=3 with chemical stimulation, n=4 with sciatic nerve stimulation). In the chemically stimulated paw, these results showed 33% more dye in the WT mice, while 30% more dye in the KO mice, on average, when compared to the non-stimulated one. However, the dye was found to be similar in the KO and the WT animals (p=0.89, 0.80 for SFP, CFP, respectively). This was also the case for the amount of dye extracted from the hind paws after electrical nerve stimulation (p= 0.05 for SHP and 0.15 for CHP). The results obtained from the hind paws after electrical nerve stimulation, however, were also confounded by different intensities used for stimulation as well as volume conduction (see more details in 3.3). In the literature, there was lack of reports using electrical stimulation for Evans blue extravasation in mice. The studies which used electrical stimulation used mostly rats so we did not use absolute values from those studies. We tested excitability of fibers with gradually increasing voltage and intensity of stimulation parameters as smaller thresholds often yielded no results. Hence, it resulted in range of stimulation parameters.

Figure 3.1 here

3.2. Differences in microcirculatory changes as measured by laser Doppler flux

The immediate response in the microcirculation after nociceptor activation could be quantified by the use of a laser-Doppler probe in 5/12 experiments. Electrical stimulation of the sciatic nerve resulted in varied flux responses in several KO animals as shown in Fig.3.2A (data

from 4 KO mice). Sometimes the flux response showed a small drop, instead of the expected increase but at intensities of 100T, most trials showed a modest increase (up to 150% of the baseline level). Data from 1 WT mouse at stimulation intensity of 50T showed repeatedly a small increase. When stimulation was at or over 100T, the flux response was significantly greater than baseline in some animals. As the illustration depicts in Fig. 3.2B, however, these large flux responses were accompanied by large CDPs – in spite of the sciatic nerve being severed. The CDPs are expected to look very different before and after cutting the sciatic nerve. As shown in Fig 3.2.C, the responses to intact sciatic nerve stimulation (black traces) grew in amplitude when the intensity was increased. However, after cutting the nerve, the CDP responses should be null (except for the early stimulus artefact, box). As shown in Fig. 3.2B, such null CDP response was evoked when 50T stimulation was used. Those instances when there was a large flux change immediately after stimulation, the CDP responses were also large (red circle in Fig. 3.2B). After systematically testing the relationship between the size of the flux response and the CDPs in 3 mice, the large flux responses were always associated with large CDP responses.

Figure 3.2 here

3.3. Differences in the Evans blue distribution measured by fluorescence imaging

From the *in vivo* small animal imaging experiments on 38 animals, data from 30 mice (14 age-matched pairs) were used for further analysis. The very first pair was used for optimizing the scanning protocol and due to some procedural differences; they were excluded from the analysis. The non-age-matched animals of the additional trials were also excluded from comparative analysis. In all pairs, images were collected for 5 minutes after the Evans blue dye injections (but prior to stimulation) and then they were recorded for another 15 minutes after stimulation has been initiated. Post-hoc analysis of the total fluorescent voxel counts (**TFC**) in the identified

ROIs and of the voxel counts with maximum fluorescence resulted in data as shown in Fig. 3.3A (from one animal). After obtaining the ratio of these readings in the ROIs over the stimulated and the non-stimulated paws, there was a consistent result with either of these measures. Notably, the signal ratios of the two ROIs were close to one over the baseline period but they started to increase within a minute after the stimulant was applied (at time 0 in Fig. 3.3.A-C). Further analysis of these measurements was done by using only the TFC values.

Figure 3.3 here

The summary of Evans blue fluorescence expressed as ratios in all age matched pairs animals (n=8) tested with 100% xylene is shown in Fig. 3.3B and C. The Evans blue fluorescence always increased after the xylene application and it always peaked by around 5 minutes after stimulation has been initiated. There was a plateau in the signal after the peak by about 7-9 minutes when followed for 15 minutes after xylene application.

Figure 3.4 here

Relying on the comparison of the EB signal between stimulated and non-stimulated paws is not an optimal measure of the peripheral responses as there are known changes in vasodilation and EV in both the stimulated and also the non-stimulated hind limb (Lobanov & Peng, 2011). In some animals, the ratio of the Evans blue in the two hind paws was already different at baseline (symbols with x in Fig. 3.3B). In order to account for these shifts, the mean change in TFCs in the stimulated hind paw as well as in the non-stimulated paw was calculated after correcting for baseline fluctuations. First, the TFCs were expressed as the percent of the maximum TFC obtained in each animal (during the 0-15 minutes period). Then the last two minutes of the baseline period were averaged and finally, the TFC readings at each time point after stimulation were subtracted from the averaged baseline value. The results after baseline correction and

normalization to maximum TFC were separately analyzed for the stimulated paw as shown in Fig. 3.4 and for the non-stimulated paw as shown in Fig. 3.5. These normalizations were done for data from the animals that received 100% xylene (Fig. 3.4A and Fig. 3.5.A), and those that received 75% xylene (Fig. 3.4.B Fig. 3.5. B) and those that received 5% formalin (Fig. 3.4.C, Fig. 3.5. C). There was no significant difference in TFC between WT and KO in stimulated paws. Between 4 and 9 minutes after xylene application, there was a larger change observed in the non-stimulated paw of the KO mice than in WT mice. The difference between the KO and WT animals was in the opposite direction when 100% and 75% xylene was applied., When 100% xylene was used, the KO animals tended to shown a significantly larger response at 12 and 12.5 minutes (p=0.04, 0.04); while with 75% xylene application, the WT animals showed a significantly greater response in the 4-9 min window (p= 0.030, 0.021, 0.003, 0.000, 0.002, 0.004, 0.01, 0.01, 0.02, 0.03, 0.03).

Figure 3.5 here

As the EB dye is being metabolically cleared after its dissipation in the venous system, it was important to determine the baseline rate of change without any stimulation applied. In order to address the immediate changes in the EB levels after nociceptor stimulation and to test whether there is an attenuated response in the KO animals, the rate of TFC was calculated based on the *in vivo* images. After normalizing the rate of change values to the maximal change evident in each animal, the averaged results showed an interesting pattern as shown in Fig. 3.6. Within the first two minutes of xylene application, the rate of change was slower in the KO animals than in the WT mice (Fig 3.6.A, p=0.03). This was also a trend in the other series as well (Fig. 3.6 B-C) but without reaching statistical significance.

Figure 3.6 here

The average rate of change in the non-stimulated paws showed overall a different, more variable pattern than the rate of change in the stimulate paws as shown in Fig. 3.7. The negative values, representing a drop in the fluorescence counts observed in the non-stimulated paws were not observed at all in the stimulated paws. This drop stopped and reversed into an increase of signal between 1.5-2 minutes following the start of stimulation. The rate of change was faster in KO mice within 1.5 minutes (Fig 3.7A, p=0.01, 0.02, 0.04).

The non-paired animals mentioned as additional trials in table 2 were used to test different stimuli (6 KO and 2 WT). Electrical stimulation of sciatic nerve was done in 1 WT and 1 KO followed by fluorescence imaging. 50% xylene diluted in mineral oil was used as an irritant in one WT, 75% xylene diluted in mineral oil was tested in 1 KO without an age matched pair. In 2 KO animals, without age matched pairs, 75% xylene diluted in ethanol was used. Besides these, two KO were used for the initial trials with 5% formalin injection without a matched pair. In some of the animals, we also tested saline's topical application in order to verify that the signal change was smaller with saline than with the irritants.

Figure 3.7 here

4. Discussion

In the studies described herein, I provide evidence for some differences in the peripheral responses to nociceptor activation between two strains of mice, one of which lacks Cx36. Most notably, this work has established a novel, *in vivo* fluorescence imaging method for testing peripheral responses to painful stimuli and validated its use for two types of stimulants (xylene and formalin) in adult mice.

4.1 Summary of results

1) Although there was a greater amount of extravasated EB dye resulting from xylene induced front paw stimulation in the WT animals than in the KO animals, this was not a statistically significant difference (Fig. 3.3A-B). Antidromic nerve stimulation-induced extravasation was also not significantly different in the two mouse lines (Fig. 3.3C).
2) Antidromic nerve stimulation-induced microcirculatory changes measured as flux by the laser Doppler probe in the hind paw did not allow for comparisons to be made between responses in KO and in WT animals due to small flux changes unless an aberrant stimulation of other nerves was also induced.
3) The novel *in vivo* fluorescence imaging method provided consistent readings of the EB signal before and after nociceptor stimulation. Only non-significant, small differences were found in terms of greater EB readings within the first 5 minutes after xylene application in the WT than in the KO animals (Fig. 3.4A-C).
4) The non-stimulated, contralateral paws also showed an increase of EB signal after stimulation. These recordings suggest a different pattern than the EB signal pattern in the stimulated paws which has not been describe previously in the pain literature with as much detail as live imaging allowed it.

4.2. Mechanisms underlying nociceptor activation by xylene, formalin

Xylene involves TRPV1 receptor stimulation. TRPV1 is a member of Transient Receptor Potential (TRP) family of cation channels and within that family it is member of vanilloid subfamily. TRPV1 ion (Ca^{2+}) channel is a 95kDa protein formed from four TRPV1 molecules. Each TRPV1 molecule has six transmembrane domains and a hydrophobic loop connecting the fifth and sixth domains. It has intracellular N and C termini. It forms a molecular complex called

transduciosome containing Protein kinase A (PKA), Tyrosine kinase A, Phospholipase Cγ (PLCγ), protein kinase Cε (PKC), phosphatidylinositol 4-5 bisphosphate (PtdPns(4,5)P2). These proteins are involved in regulation of channel activity such that PKA and PKC increases the channel activity by phosphorylating it whereas PLCγ hydrolyzes PtdPns (4,5)P2 that further inhibits TRPV1 channel (Jancso, 2009). Activation of this channel causes the pore to open and causes Ca^{2+} influx. This influx depolarizes the neuron and generates an action potential (Szallasi & Blumberg, 1999). In knockout mice for TRPV1, no nociceptive behavior (such as paw liftings and shakings) was seen on xylene exposure (Sándor et al., 2009). Only 30% of the xylene-induced EV remained in TRPV1 knockouts vs the response in the WT line (Sándor et al., 2009).

Xylene also evokes a long term inflammatory response that is considered to be independent of TRPV1 channel but mediated by TRPA1 channel (Caterina et al., 2000). TRPA1 is an excitatory cation channel in the TRP family. Topical application of xylene causes tissue injury and cellular stress leading to the generation of reactive oxygen species (ROS). ROS further leads to the production of carbonylated proteins which are responsible for activating TRPA1 channel. Opening of TRPA1 causes Ca^{2+} influx and release of neuropeptides such as substance P (SP), Calcitonin Gene Related Protein (CGRP), neurokinin A (NKA) at the peripheral ends of sensory nerves. SP binds to the tachykinin receptors NK1 on vascular endothelial cells and causes plasma extravasation. CGRP induces vasodilation and enhances SP induced extravasation (Trevisani et al., 2007). EV was less affected by SP than vasodilation according to Lembeck and Holzer 1979 (Lembeck & Holzer, 1979).

4.3. Methodological considerations for the interpretation of the results

The Cx36 protein may be present in not only those DRG neurons innervating the skin but also those innervating other tissue like muscle or internal organs; but our tests were limited to the

examination of those that innervate the legs. The reason we choose skin of the foot pad to test was because this has the highest amount of EV relative to other body parts (Pinter & Szolcsanyi, 1995).

The age of the mice varied greatly in this study (see Table 1). The way we took into account the age of the animals was by the age matching and also by applying the paired t-test for examining differences between age matched WT and KO pairs in each series. Another statistical method, the so called repeated measures analysis of variance (rmANOVA) would have been also an appropriate choice here. The rmANOVA has been used earlier in the evaluation of the EV time course study by Gonzalez *et al*. (Gonzalez et al., 2005). The rmANOVA could also take two factors, the presence of Cx36 and the age, into account. This is a "less stringent" test in terms of establishing significance levels when compared to the paired t-test, and potentially this would have resulted in more differences than the ones established by the t-test.

The activation of the sympathetic preganglionic neurons by the painful stimuli results in vasoconstriction at the site of injury that is competing with the vasodilation induced by other mechanisms. By blocking the autonomic nervous system, confounding factors related to peripheral vasoconstriction can be removed. Earlier research work pertaining to peripheral responses after nociceptor stimulation have blocked autonomic responses by using guanethidine, a ganglion blocker, and thereby induced "chemical sympathectomy" (Gamse & Saria, 1987; Lembeck & Holzer, 1979). Blocking of sympathetic input, however, has been found to have very small or no effects on EV (Donnerer et al., 1991). Therefore, we did not block autonomic responses when applying xylene or formalin.

As mentioned in the Introduction, xylene and formalin are known to induce concentration dependent EV. In this study, we used 100% and 75% xylene. The reason for using the 75%

strength was to investigate whether there is a slower time course and/or an attenuated response when compared to 100%. The attenuated response is based on the premise that the lower concentration of the irritant would have affected a smaller area initially and the flare (mediated by the Cx36) would be more evident than with the higher concentration solution. The number of animals we tested did not support this, but a larger sample size is necessary to reach a conclusion. Another factor to be considered is that the differences between 100% and 50% xylene-induced responses (measured as number of paw lifts) have been found to be strain dependent. While in BalbC mice no significant differences were found between the responses induced by 50% and 100% xylene, the C57BL/6 strain showed significantly lower number of paw lifts in response to 50% than to 100% xylene (Sándor et al., 2009).

The use of two different nociceptive stimuli – the electrical and the chemical - in the same animal during the same experiment was a choice we made in order to obtain more data during the *in vivo* electrophysiology experiments than it would have been possible by applying only one stimulant. The use of more than one stimulus could have confounded our results because of interactions between the left and right sides. The effects of electrical stimulation of cut dorsal roots, nerves or of chemical stimulation have been studied on plasma EV and vasodilation in both ipsilateral and contralateral hind paws (Lobanov & Peng, 2011; Pinter et al., 1996). Contralateral plasma EV was also described in pelvic organs after unilateral stimulation of dorsal roots (Pinter & Szolcsanyi, 1995). Regardless of how the nociceptors were activated, vasodilation and EV often occur on both sides. Some evidence also suggested that antidromic electrical stimulation of lumbar dorsal roots has anti-inflammatory effects on the contralateral paw (Pinter & Szolcsanyi, 1996; Szolcsányi et al., 1998). The interactions between forepaw and

hind paw could be similar to the interactions between the two sides but we haven't found any studies investigating this possibility.

In order to induce EV by antidromic stimulation, constant current stimulation with square pulses of 3 mA and 0.5 ms duration at 4 Hz or 8 Hz is necessary for a minimum of four minutes in the rat (Carmichael et al., 2008). The EV response plateaus and there is no additional response with more pulses or with stronger currents. Stringent electrical stimulation parameters for each animal with the above listed parameters for four minutes would have been the most optimal electrical stimulation paradigms in this study.

Due to known sex differences in EV, we focused mainly on examining male mice. Testosterone and estrogen have opposing effects on neurogenic EV (Flake et al., 2006) and corticotropin releasing factor also impacts neurogenic EV (Wei et al., 1986). There is sexual dimorphism when responding to "stress or painful stimulation" inherent in the inflammatory response manifesting as different levels of EV see e.g. (Green & Levine, 2005). Typically males are the choice for studies pertaining to EV, but these were mainly based on experiments with rats as mice have been less frequently used for electrical stimulation induced EV protocols. The type of stimuli applied to nociceptors can also dictate whether there is a sexually dimorphic response or not. For example, females have a greater inflammatory response when inflammation is induced by capsaicin and noxious heat; suggesting possible sex-related changes in TRPV-1 receptor mediated mechanisms (Carmichael et al., 2009).

4.4. The complexity of the Evans blue signal

The extravasated EB dye is in a sense an "end" result of a pain response. The pain responses initiated by chemical stimuli have been recognized as biphasic responses with an early and a late component. The early response is manifested in behavior such as flinching, lifting of

the paw and it lasts for a few minutes. The late response starts at 10 minutes after stimulation and it lasts for 30-45 minutes (Dubuisson & Dennis, 1977; McNamara et al., 2007). The early response occurs because of C fiber activation by the stimulus and the late response is mainly the result of inflammatory reactions due to the release of inflammatory mediators (McNamara et al., 2007; Tjolsen et al., 1992). The EV that we measured during *in vivo* electrophysiology experiments was the late response in most of our animals as the xylene was applied for longer than 10 minutes (Table 1). Our results could have been different if we had stopped at 10 minutes after xylene application in each animal and those measurements would have reflected the early response.

Increased flux responses has been consistently seen before in rat hind paw skin when the sciatic nerve was electrically stimulated (Gamse & Saria, 1987). The proposed use of the laser doppler method for measuring flux in a select hind paw area has been difficult at first as there was no prior report on how to stimulate a nerve or how to interpret any flux changes during similar procedures in mice. We stimulated at various intensities but the flux showed no discernable change until very high voltages were used. The flux change only occurred at electrical stimulation intensities well above the strength required for C-fiber activation. Accidentally we noticed in one animal that our CDP recordings were depicting a response as if the sciatic nerve was intact when a large flux change was present. After this observation, we systematically tested in three animals the CDP response before and after cutting the sciatic nerve and examined when spread of electrical stimuli occurred. The electrical stimulation aimed to activate the cut sciatic nerve, however, spread onto a larger area was observed when the applied voltage was high. This would have induced the so called volume conduction effect. In this context, volume conduction refers to the electrical current stimulating another intact nerve, such

as the femoral nerve in the hind leg. Therefore, action potentials from the intact nerve would have resulted in a central response and not only a peripheral response, as expected if only the cut sciatic nerve would have been stimulated. There is no mention of volume conduction as a confounding factor when assessing flux changes, as far as we could tell after an extensive literature review. This however, could be due to the fact that originally, antidromic EV was induced by cut sciatic stimulation that was placed in a chamber (Jancso et al., 1967) and these previously applied procedures were also performed in larger animals. The currents can be larger before they spread in large animals when compared to the mouse, where the distances between different nerves are relatively much smaller than in a cat or a rat. It was an unexpected finding, however, that no obvious flux changes could be evoked even though our stimulation was strong enough to recruit C-fibers; or in many trials, even far beyond the C-fiber recruitment threshold. One possibility is that other previously recorded large flux changes by nerve stimulation actually represented changes due to volume conduction and electrical stimulation of all tissue (and not only C-fibers). Alternatively, another possibility is that in the mouse paw, our probe was placed over an area that does not respond in terms of microcirculatory changes after sciatic nerve stimulation.

The *in vivo* fluorescence imaging signal represents a mixture of extravasated EB and the EB present in the circulation at each time point. Furthermore, this signal is also influenced by the clearance of the EB from the body. The 5 minute baseline imaging was based on a previous study which used digital imaging analysis of paw photographs (Gonzalez et al., 2005). However, based on our results, a longer - about 7-8 minute baseline would have been perhaps a better choice with more stable "initial" levels of the EB dye as there was still a drop in the EB signal in some of our series after 5 minutes wait. The baseline correction method we applied was the

same as the method used by Gonzalez *et al.* 2005; thus our data can be compared to their results. There is good correspondence of the peak of the EB EV and the time course of the EV between our and their experiments.

The negative values of the rate of change in the non-stimulated paws were not observed in the stimulated paws. These drops could be reflecting the clearance of the EB from the hind limb via the circulatory system and the lack of vasodilation and EV in that paw. The EV in the contralateral side to the stimulation is known to occur, but its time course has not really been defined, to our knowledge. The data set collected from the imaging series is the first to report contralateral changes so close to the time of stimulation and thereby it requires further comparisons between different stimulants. These observations, however, may reflect how fast different types of nociceptors can recruit other afferents contralateral to the stimulated side. This translates to systemic effects of a pain response, as may be occurring during complex regional pain syndrome.

4.5. Physiological significance of Cx36 in peripheral nerves

As described briefly in the introduction, this study has been intended to follow the anatomical account of Cx36 in small DRG neurons in order to identify its functional role. The results obtained in this study showed that in the long term, i.e. >10 minutes after nociceptor activation, there are no differences in the EB signal between the two lines of animals. The marginal differences identified here point to the fact that early on, within 2 minutes of nociceptor activation, there is a slower response when Cx36 is absent. The most interesting similarity between the findings of the anatomical study and this study is that neurons responding to heat stimulus -identified by the TRPV1 marker - contained the most Cx36 (Zhao et al., 2015) and here, the TRPV1 receptor activation by 100% xylene induced a faster rate of change in those

animals that bear Cx36. The role of Cx36 could be relatively different based on what receptors are activated. More experiments are necessary to confirm this and the possibility that Cx36 influences pain behavior in addition to EV.

4.6. Future directions

In addition to quantifying EV, behavioral pain responses of WT and KO mice measured as paw lifts, lickings or tail flinch could be compared in future studies. Especially in the early phase, the KO animals are expected to show fewer responses than the WT animals, if the EV results also correlate with pain behavior. Testing of mechano-sensitive nociceptors activation, for example by pin prick, could also be a useful method during *in vivo* fluorescence imaging. The pin prick evokes a localized injury over a small, defined region and the spread of the flare could be more obvious than in the case of a chemical stimulant potentially spreading far from the area where it was applied (in spite of the small volume used). There would be great merit in performing comparative studies with the pin-prick during *in vivo* small animal imaging. This is also important in the light of different relative amounts of Cx36 in the different types of small neuron (Zhao et al., 2015). Focusing on smaller regions on the paw should also be attempted during *in vivo* small animal imaging. The resolution used here was chosen to be optimal for image both hind paws but at the same time, this meant a loss of sensitivity in terms of zooming into small regions around the initially stimulated site. Differences made to the flare in the triple response would be more likely detectable if the spatial resolution around the stimulated region is high.

In terms of Cx36 facilitating the axon reflex, stringent studies are yet to be performed that could answer the possibility that the presence of Cx36 also correlates with more electrical coupling between nerve fibers. The key for those studies will be to stimulate nerve branches

innervating the same or neighboring receptive fields. Initially, this was attempted in combination with the EV during the *in vivo* electrophysiological studies reported here; however, a separate series of experiments dedicated only to record axon reflexes would be necessary. Anatomical evidence for branching of sensory nerves so that some innervate vessels and some innervate skin has been presented earlier (Chapman & Goodell, 1964; Helme & McKernan, 1985) but the role of the different branches and the possibility of antidromic passage has been questioned by a few researchers. For example, as the receptive field of a sensory nerve is almost the same as the extent of the flare; it refutes that there is any branching at all (Lisney & Bharali, 1989). The most compelling evidence for coupling between not only peripheral branches of the nerve fibers but also potentially between those running parallel in a peripheral nerve come from studies in the baboon (Meyer et al., 1985). These experiments would have to be repeated in the WT and KO mice; but the size of the sural nerve in the mouse makes these experiments challenging.

5. Conclusions

This study aimed to quantify the contribution of Cx36 to plasma extravasation responses following stimulation of nociceptors by examining responses in WT and KO mice after the application of noxious stimuli (xylene, formalin, electrical stimulation of the sciatic nerve). Extravasation of EB dye from the circulation in the limbs was evaluated by spectrophotometry, laser Doppler flux and *in vivo* fluorescence imaging. A trend for marginally greater responses as well as for a faster rate of change in the EB fluorescence was found within the first 2 minutes after xylene application in WT than in KO mice. This enhanced early vascular response in the WT animals compared to the KO animals is consistent with earlier reports of electrical coupling present between C-fibers. The anatomical presence of Cx36 in small sensory neurons, therefore, can be correlated with a role in the EV phase of the triple response. A novel, *in vivo* EB

fluorescence imaging-based method for evaluation of peripheral responses to painful stimuli has been validated by this study and its use for two types of stimulants (xylene and formalin) has been established in adult mice.

Table 1. *In vivo* electrophysiology experiments

Series	Cx36 WT	Weight (g)	Age (days)	Sex	Xylene stimulation (mins)	Cut Sciatic stimulation (mins)	Cx36KO	Weight (g)	Age (days)	Sex	Xylene stimulation (mins)	Cut Sciatic stimulation (mins)
Sciatic nerve electrical stimulation and xylene	EV 9	26	91	M	55	37	EV 7	23	91	M	106	106
	EV 1	45	232	M	76	20	EV 10	41	231	M	47	47
	EV 2	43	234	M	72	29	EV 11	38	234	M	62	62
	EV 3	42	238	M	53	27	EV 12	39	247	M	38	38
							EV4	21	232	M	NA	NA
							EV 5	34	184	M	29	29
							EV 6	20	89	M	11	11
							EV08	23	98	M	NA	NA

Table 1. Details of the experimental series that tested sciatic nerve electrical stimulation and xylene on the WT (n=4) and KO (n=8) animals. There were four age matched pairs and 4 KO animals without age matched pair. The animals' weight (in grams), age (in days) and sex is listed here as well as the time for which xylene was topically applied (minutes) and the time for which the cut sciatic nerve was stimulated (minutes).

Table 2. *In vivo* small animal imaging experiments

Series	Cx36 WT	Weight(g)	Age (days)	Sex	Cx36KO	Weight(g)	Age (days)	Sex
100% Xylene n=18	IVI W1	23	298	F	IVI K1	35	298	F
	IVI W2	32	142	F	IVI K2	23	142	F
	IVI W3	27	144	F	IVI K3	21	144	F
	IVI W4	23	59	M	IVI K4	20	59	M
	IVI W5	26	68	M	IVI K5	22	66	M
	IVI W6	20	77	F	IVI K6	20	78	F
	IVI W7	18	77	F	IVI K7	21	78	F
	IVI W8	39	140	M	IVI K8	37	140	M
	IVI W9	34	127	M	IVI K9	29	125	M
5% Formalin n=6	IVI W10	20	35	M	IVI K10	21	43	M
	IVI W11	18	37	M	IVI K11	19	44	M
	IVI W12	21	37	M	IVI K12	22	45	M
75% Xylene (Mo) n=6	IVI W13	23	65	M	IVI K13	25	68	M
	IVI W14	25	70	M	IVI K14	25	73	M
	IVI W15	23	77	M	IVI K15	25	80	M
Additional trials n=8	S/75% Xylene (Mo)/100% Xylene				IVI K16	27	143	F
	S/75% Xylene (Ethanol)				IVI K17	23	143	F
	S/75% Xylene (Ethanol)/100% Xylene				IVI K18	22	144	F
	Formalin 5%				IVI K19	24	144	F
	Formalin 5%				IVI K20	22	145	F
	Electrical stimulation				IVI K21	20	145	F
	IVI W15	39	235	M	S/50% Xylene (Mo)/100% xylene			
	IVI W16	28	91	M	Electrical stimulation			

Table 2. Details of the *in vivo* small animal imaging experimental series that tested xylene (100% and 75% concentration) and formalin (5% concentration) on the WT (n=16) and KO (n=21) animals. 100% xylene was used as stimulant in 9 age matched pairs, 75% xylene (diluted in mineral oil, Mo) was tested in 3 age matched pairs, 5% formalin was injected as a stimulant in 3 age matched pairs. Some additional trials (n=8) were done to test other different stimuli: saline (S), 50% xylene diluted in Mo, 75% xylene diluted in Mo or Ethanol, 5% formalin and electrical stimulation of sciatic nerve.

6. Figures

Figure 1.1.

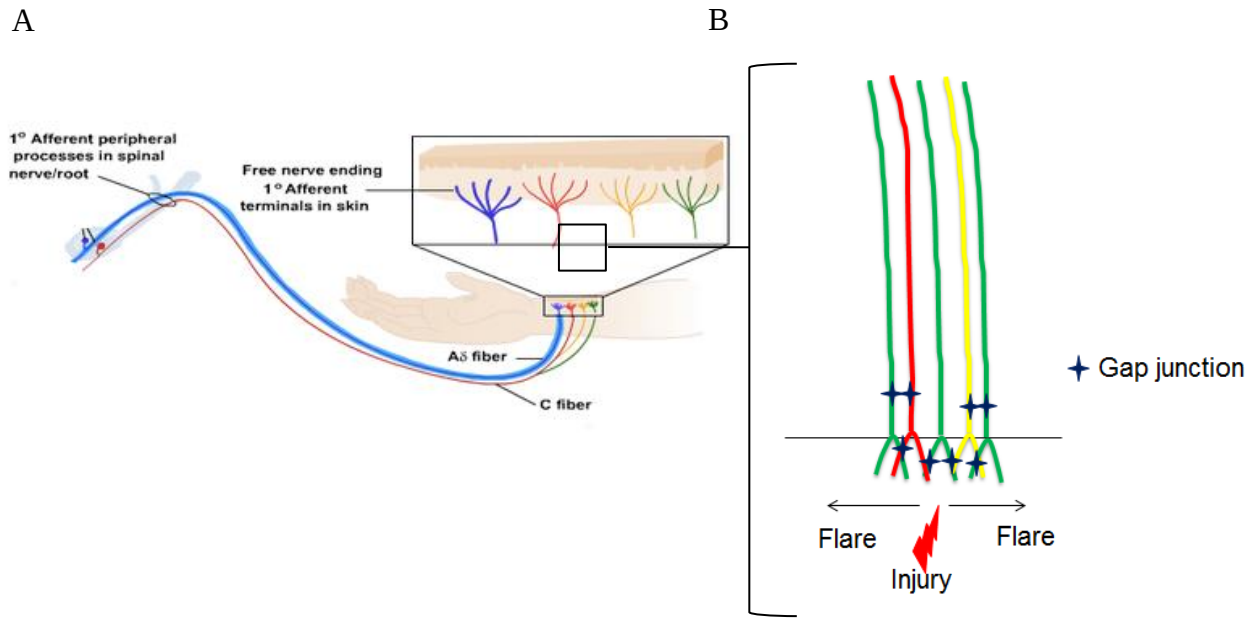

Figure 1.1. Schematic illustration of Cx36 present in peripheral nerves and its contribution to the triple response.

A. The illustration depicts the peripheral nerves with their free endings innervating the skin of the hand. Unmyelinated C fibers (red, yellow, green) and Aδ fibers (blue) are afferents involved in nociception. Our focus here is on unmyelinated C fibers. Cx36 is present in neurons of the dorsal root ganglia and it allows the formation of functional gap junction at the periphery, near the receptor ending of the afferents.

B. During the phenomenon of triple response, Cx36 gap junctions couple nociceptors and help in spreading nerve impulses to the neighboring fibers and hence, facilitate flare. The resulting response is increased vasodilation and vascular permeability. In the absence of Cx36, there is reduced vasodilation and plasma extravasation hypothesized.

Figure 2.1.

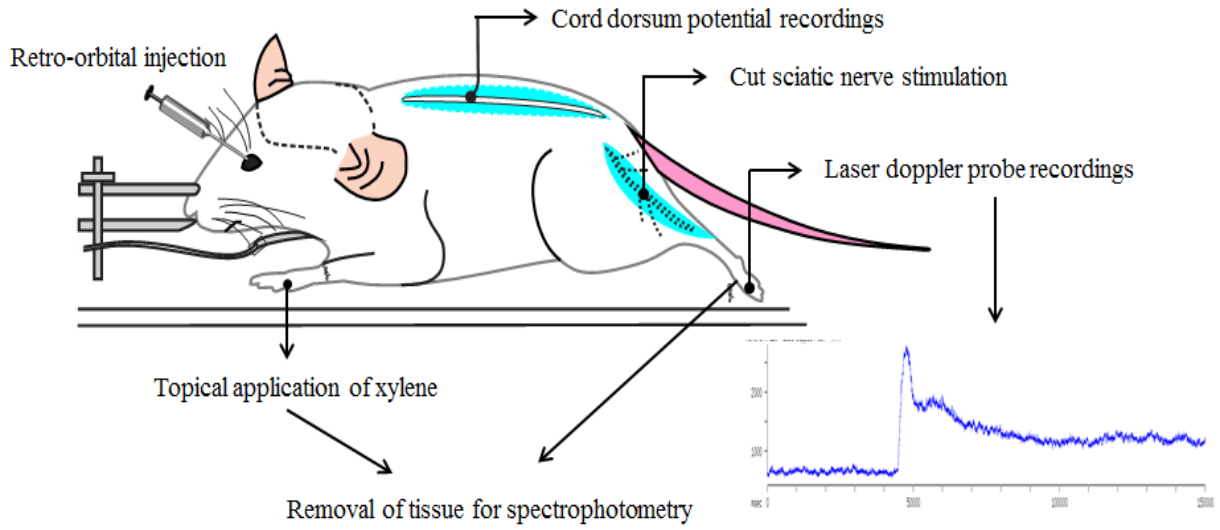

Figure 2.1: Mouse preparations for *in vivo* electrophysiology experiments

This illustration highlights the animal model (anesthetized mice on isoflurane and on ventilator) with the recordings and stimulation sites used here. Once the mouse was on ventilator, laminectomy (between T13 and L1) was done to expose the spinal cord for cord dorsum potential recordings. Sciatic nerve of the left hind leg was dissected free. Laser Doppler probe was placed below the 5^{th} digit of the left hind paw that was electrically stimulated. After the retro-orbital injection of Evans blue, xylene was applied on one front paw and the exposed sciatic nerve was stimulated. The trace (blue) exemplifies recordings collected from the probe. At the end of the experiment after trans-cardial perfusion, skin from all the four paws was removed for spectrophotometry.

Figure 2.2.

A B

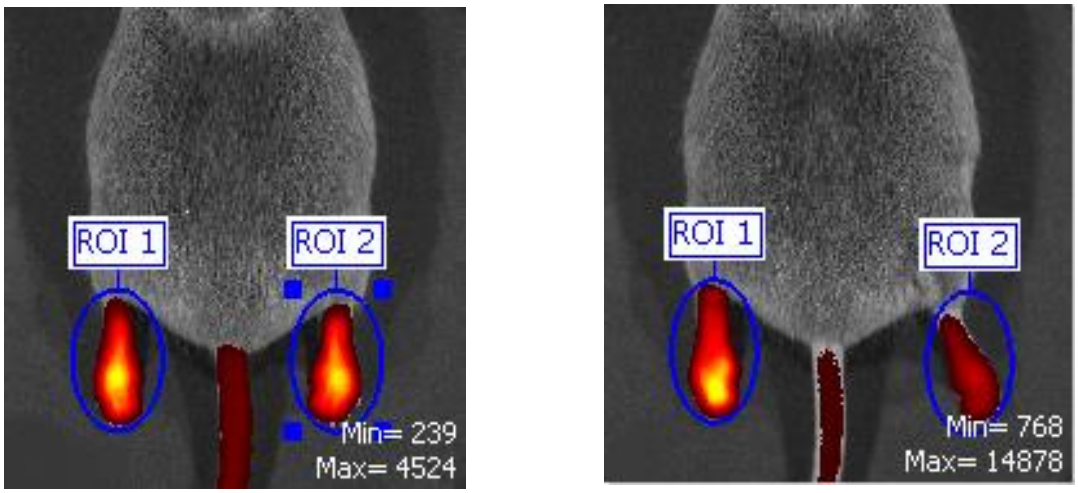

Figure 2.2. Evans Blue fluorescence *in vivo* imaging

Photographic images of the back and the hind paws from a male (66 days old) mouse were superimposed on fluorescent voxel measurements. Fluorescent images were collected for 5 minutes after retro-orbital injection of Evans Blue dye **(A)** and for 15 minutes after topically applying a chemical stimulant (15 µl, 100% xylene) on the left hind paw **(B)**. The circled areas called the region of interests (ROIs) were used for analysis of fluorescent signal quantification (area 1 on non-stimulated paw and 2 on stimulated paw; equal sizes). The images also show the minimum and maximum fluorescent counts detected and note that the counts increased after the stimulus was applied (B). The color code in the ROIs represents fluorescence intensity; the yellow color indicating highest fluorescence (normalized to the maximum count in each period).

Figure 2.3.

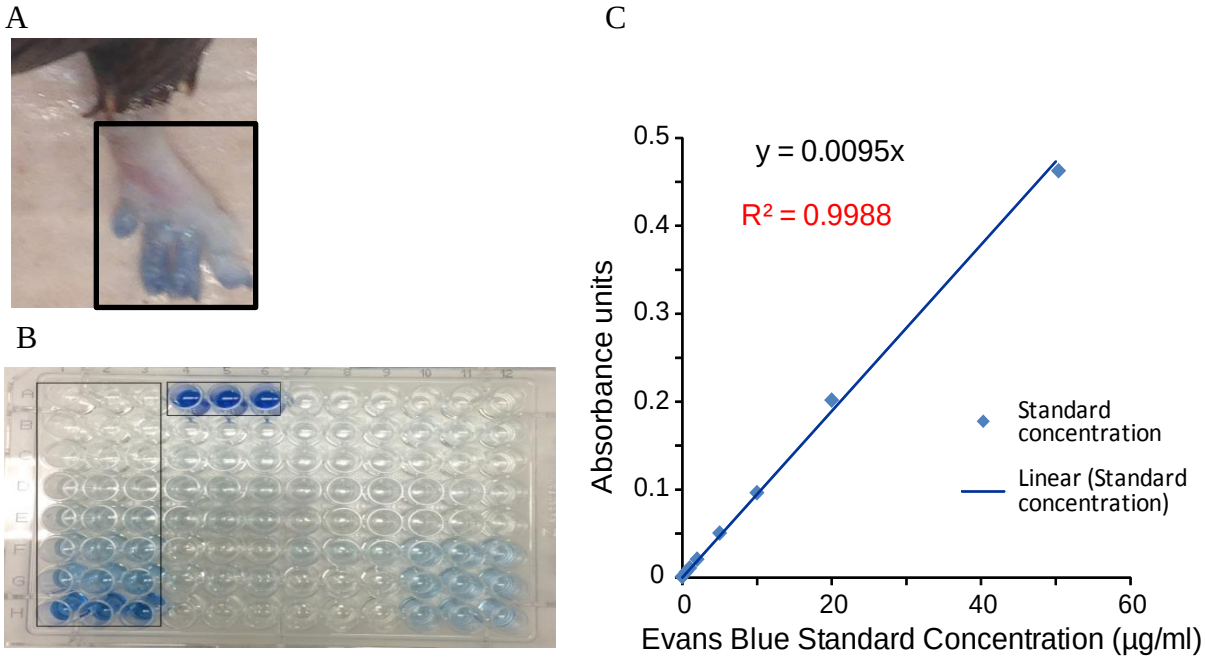

Figure 2.3. Methods used to quantify extravasated Evans Blue dye

A. Photographs of a mouse hind paw after the retro-orbital injection of Evans blue dye and electrical stimulation of the cut sciatic nerve (5 times the intensity required for the most excitable fibers, 0.2ms pulse at 20 Hz for 45 min). The square shows the skin that was removed after transcardial perfusion.

B. Well-plate used for spectrometric analysis with extracted skin samples (100 µL/well) and the standard dilutions (0, 0.5, 1, 2.5, 10, 20, 50 µg/mL) set up in triplicates (boxed areas).

C. The graph illustrates the obtained standard curve: Evans blue dye concentration (µg/mL) on the X-axis and absorbance units (nm) on Y-axis. The equation fitted to the curve (y=0.0095x) was used to calculate the absolute values of the dye in each sample (µg/mL). These values were then averaged from the triplicates for each paw of each animal and normalized by the weight of the wet skin tissue originally collected from each paw of each animal.

Figure 3.1.

A

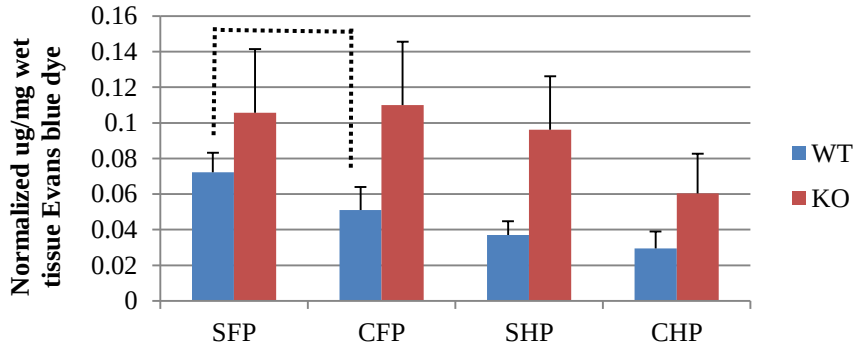

B

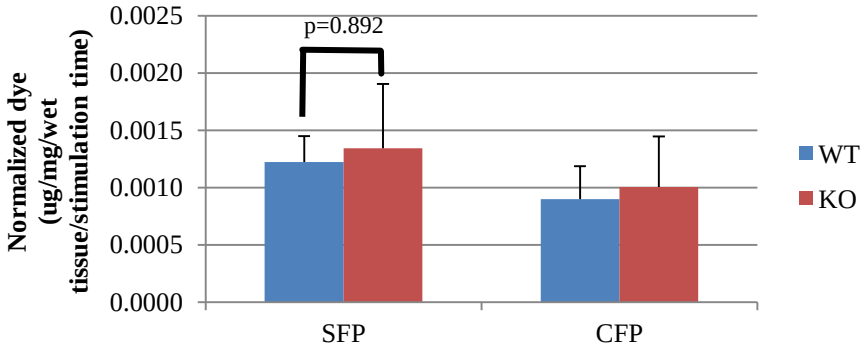

C

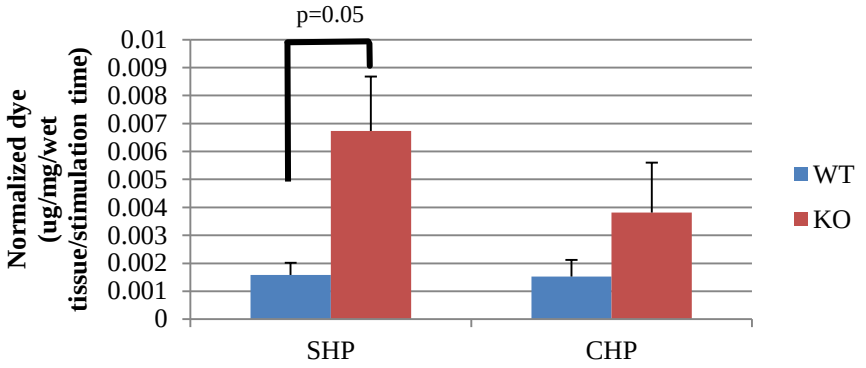

Figure 3.1. Evans Blue quantification in skin covering mouse paws

A. Extravasated Evans blue dye (µg/mg/wet tissue) in all four paws of wild type (n=4) and Cx36 knockout mice (n=6) obtained from the spectrometric analysis with triplicates for each sample.

B. Normalized Evans blue dye (µg/mg/wet tissue/stimulation time) found in the stimulated front paw from 3 pairs of age-matched animals.

C. Normalized Evans blue dye (µg/mg/wet tissue/stimulation time) found in the stimulated hind paw from 4 pairs of age matched animals. Bars represent standard error of mean (SEM) of the samples in all panels.

Figure 3.2.

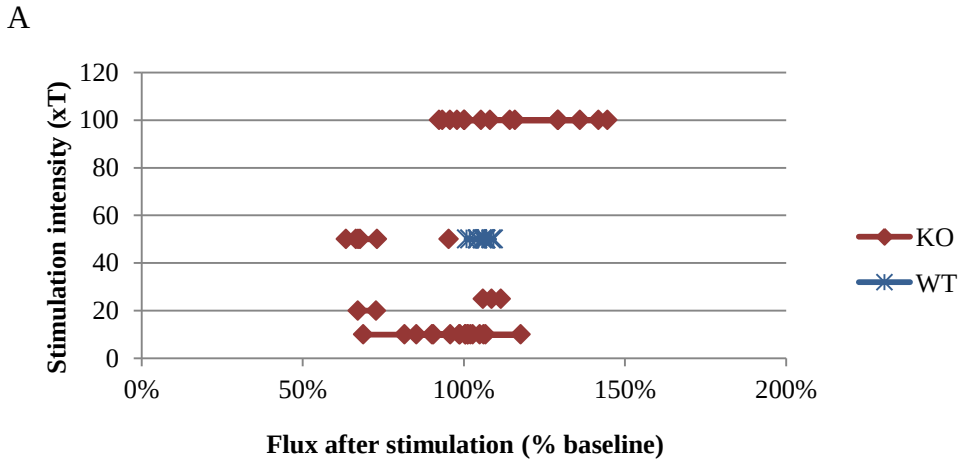
A
Stimulation intensity (xT)
120
100
80
60
40
20
0
0%
50%
100%
150%
200%
Flux after stimulation (% baseline)
KO
WT

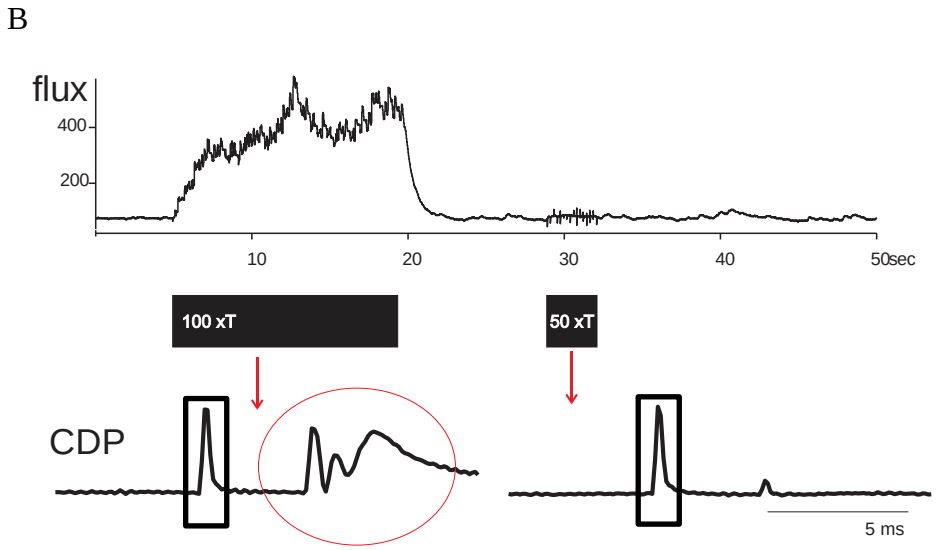
B
flux
400
200
10
20
30
40
50sec
100 xT
50 xT
CDP
5 ms

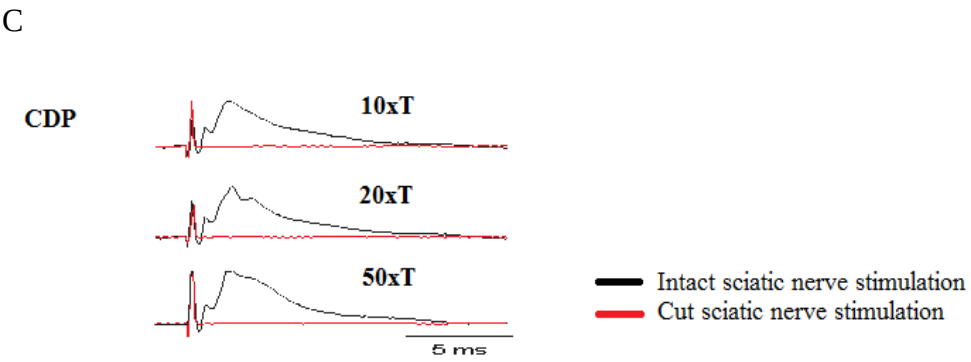
C
CDP
10xT
20xT
50xT
5 ms
Intact sciatic nerve stimulation
Cut sciatic nerve stimulation

Figure 3.2. Laser doppler measurements at various stimulation intensities

A. Laser doppler probe was used to look at immediate changes in the microcirculation after stimulation has been applied. The flux response is shown as the percent change in the area measured at baseline i.e. non-stimulated conditions from five animals (4KO/1WT).

B. When the flux response was systemically tested, large flux response was present at higher intensities but it was accompanied by large CDP responses. At 100X T there is a large flux response, and the CDP response is large (red circle) too. The CDP response should not be there as the sciatic nerve is cut proximally. At 50X T, there was no CDP response i.e. the stimulus was localized to the cut sciatic nerve but there was no large flux change either.

C. CDP recordings at different stimulation intensities (10X, 20X, 50X T) examplifying the typical response (one KO animal) when the sciatic nerve is intact (black traces) and when the sciatic nerve is cut and there is no spread of the electrical stimulus to other nerves (red traces).

Figure 3.3.

A

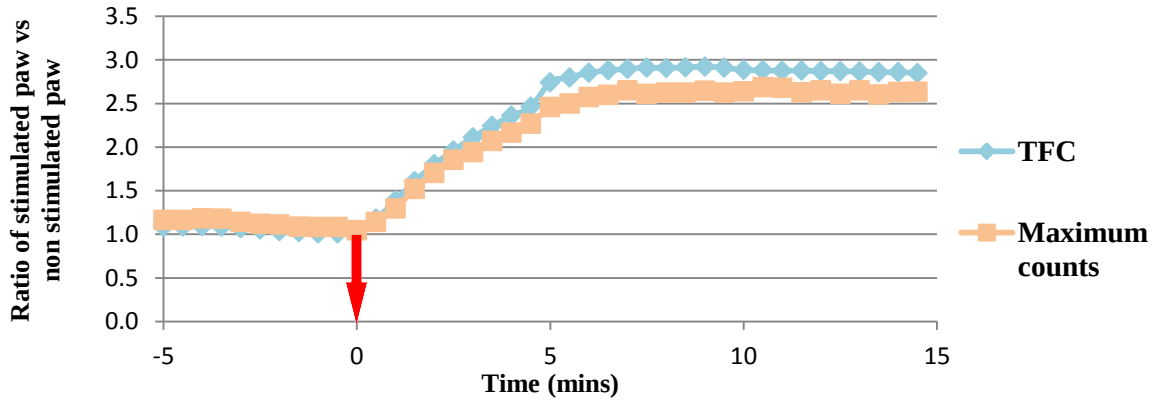

B

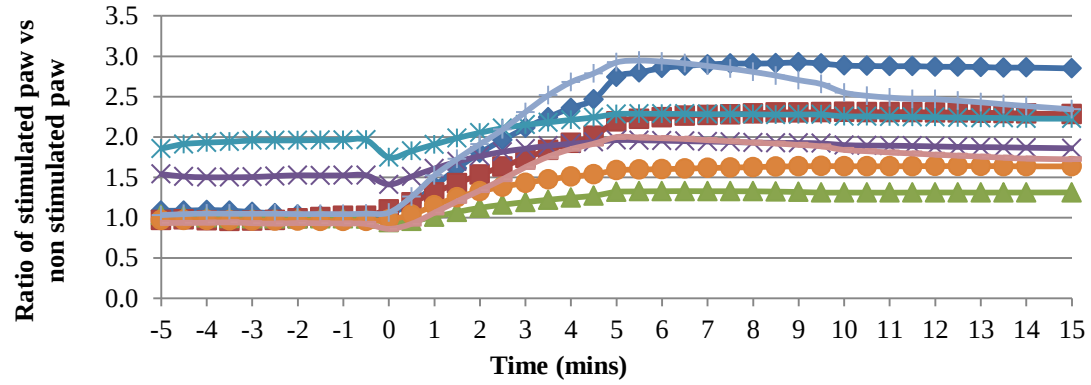

C

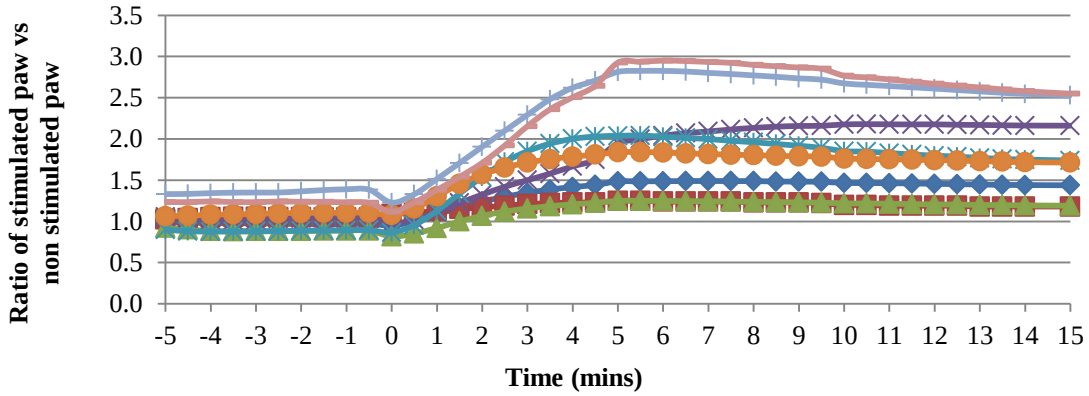

Figure 3.3. Ratio of *in vivo* Evans blue fluorescence measurements

A. The ratio of total counts of fluorescent voxels and maximum counts measured after the injection of Evans blue into the venous circulation in the stimulated vs the non-stimulated paws. Data are shown for a period of 15 minutes after the xylene (100%, 15µL) was applied (red arrow).

B-C. The ratio of total fluorescent voxels/counts in the stimulated vs non-stimulated paws of 8 WT **(B)** and 8 KO **(C).** The 0 marks the time for xylene application.

Figure 3.4.

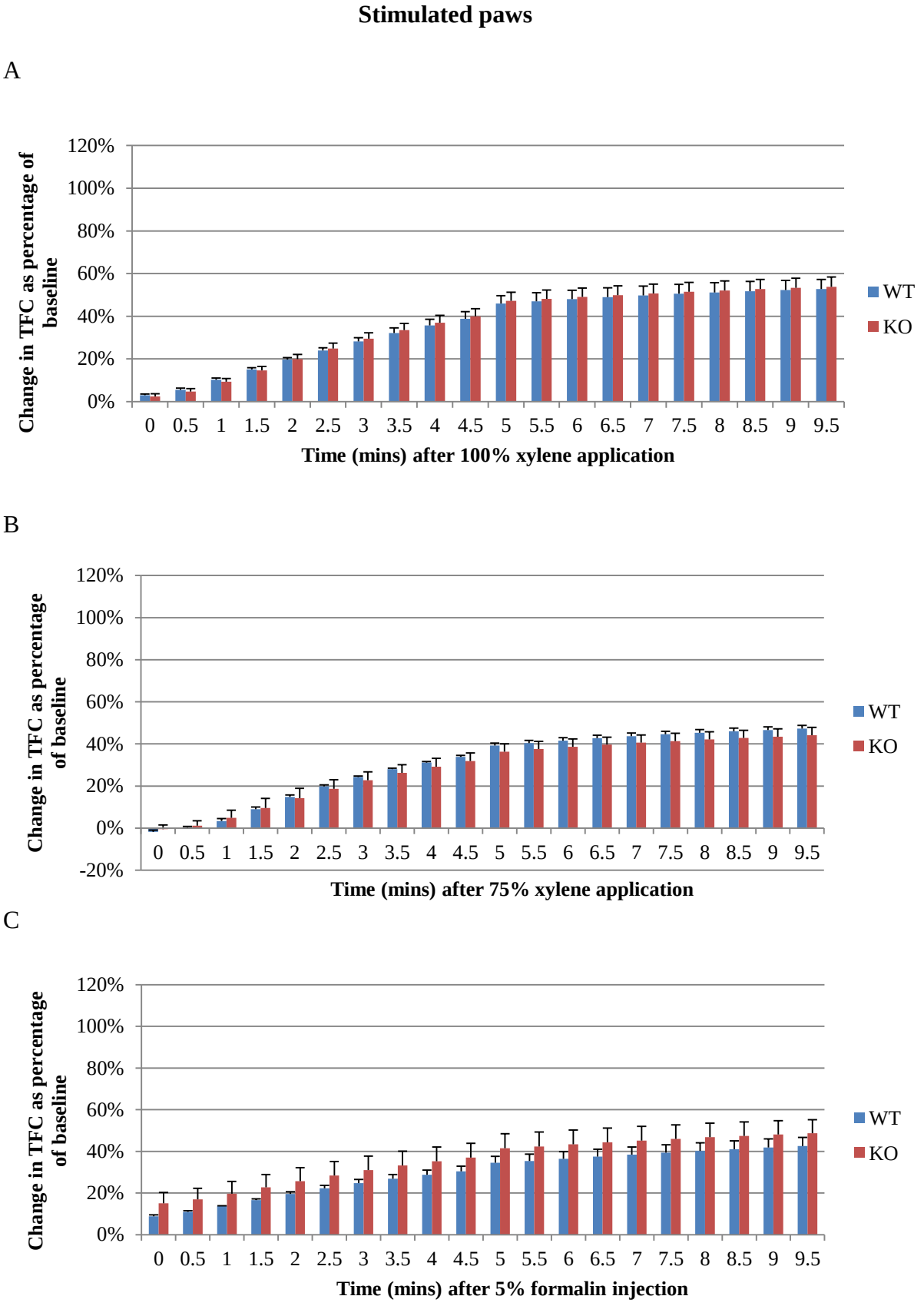
Stimulated paws
A
Change in TFC as percentage of baseline
120%
100%
80%
60%
40%
20%
0%
0 0.5 1 1.5 2 2.5 3 3.5 4 4.5 5 5.5 6 6.5 7 7.5 8 8.5 9 9.5
Time (mins) after 100% xylene application
WT
KO
B
Change in TFC as percentage of baseline
120%
100%
80%
60%
40%
20%
0%
-20%
0 0.5 1 1.5 2 2.5 3 3.5 4 4.5 5 5.5 6 6.5 7 7.5 8 8.5 9 9.5
Time (mins) after 75% xylene application
WT
KO
C
Change in TFC as percentage of baseline
120%
100%
80%
60%
40%
20%
0%
0 0.5 1 1.5 2 2.5 3 3.5 4 4.5 5 5.5 6 6.5 7 7.5 8 8.5 9 9.5
Time (mins) after 5% formalin injection
WT
KO

Figure 3.4. Mean change in total fluorescent counts in the stimulated hind paws

A. Mean change in total fluorescent counts in stimulated paws after 100% xylene applied on the hind paw (8 pairs).

B. Mean change in total fluorescent counts in stimulated paws after 75% xylene applied on the hind paw (3 pairs).

C. Mean change in total fluorescent counts in stimulated paws after 5% formalin injected in the hind paw (3 pairs).

The 0 marks the time for xylene application, error bars represent Standard Error of Mean (+SEM).

Figure 3.5.

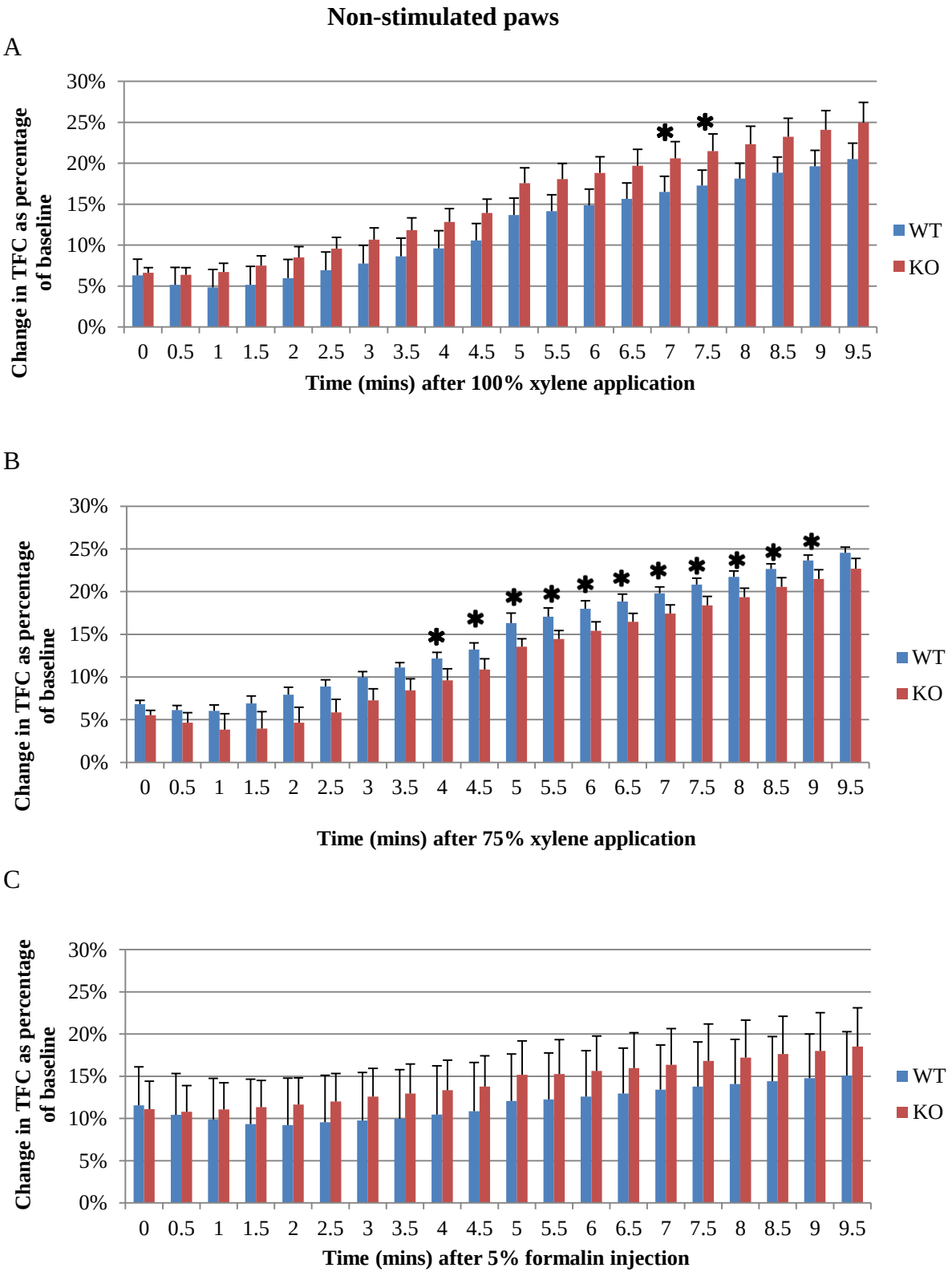
Non-stimulated paws
A
Change in TFC as percentage of baseline
30%
25%
20%
15%
10%
5%
0%
0 0.5 1 1.5 2 2.5 3 3.5 4 4.5 5 5.5 6 6.5 7 7.5 8 8.5 9 9.5
Time (mins) after 100% xylene application
WT
KO
B
Change in TFC as percentage of baseline
Time (mins) after 75% xylene application
C
Change in TFC as percentage of baseline
Time (mins) after 5% formalin injection

Figure 3.5. Mean change in total fluorescent counts in the non-stimulated hind paws

A. Mean change in total fluorescent counts in non-stimulated paws after 100% xylene applied on the hind paw (8 pairs).

B. Mean change in total fluorescent counts in non-stimulated paws after 75% xylene applied on the hind paw (3 pairs).

C. Mean change in total fluorescent counts in non-stimulated paws after 5% formalin injected in the hind paw (3 pairs).

The 0 marks the time for xylene application, error bars represent Standard Error of Mean (+SEM).

Figure 3.6.

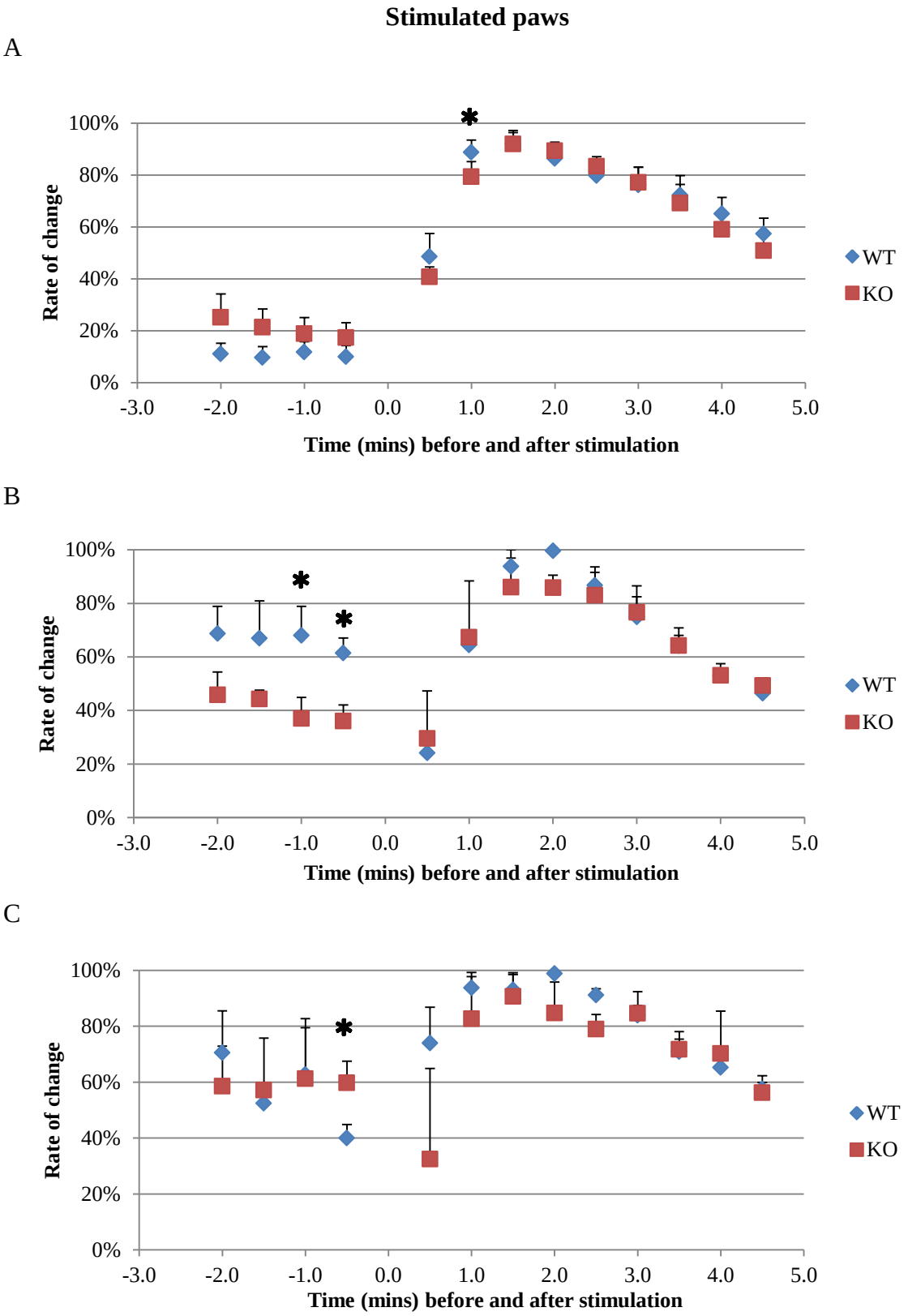
Stimulated paws
A
100%
80%
60%
40%
20%
0%
Rate of change
-3.0
-2.0
-1.0
0.0
1.0
2.0
3.0
4.0
5.0
Time (mins) before and after stimulation
WT
KO
B
100%
80%
60%
40%
20%
0%
Rate of change
-3.0
-2.0
-1.0
0.0
1.0
2.0
3.0
4.0
5.0
Time (mins) before and after stimulation
WT
KO
C
100%
80%
60%
40%
20%
0%
Rate of change
-3.0
-2.0
-1.0
0.0
1.0
2.0
3.0
4.0
5.0
Time (mins) before and after stimulation
WT
KO

Figure 3.6. Average rate of change in stimulated hind paws

A. Average rate of change in total fluorescent counts in the stimulated paws before and after 100% xylene was applied topically (8 pairs).

B. Average rate of change in total fluorescent counts in the stimulated paws before and after 75% xylene was applied topically (3 pairs)

C. Average rate of change in total fluorescent counts in the stimulated paws before and after 5% formalin was injected (3 pairs).

The 0 marks the time for xylene application, error bars represent Standard Error of Mean (+SEM).

Figure 3.7.

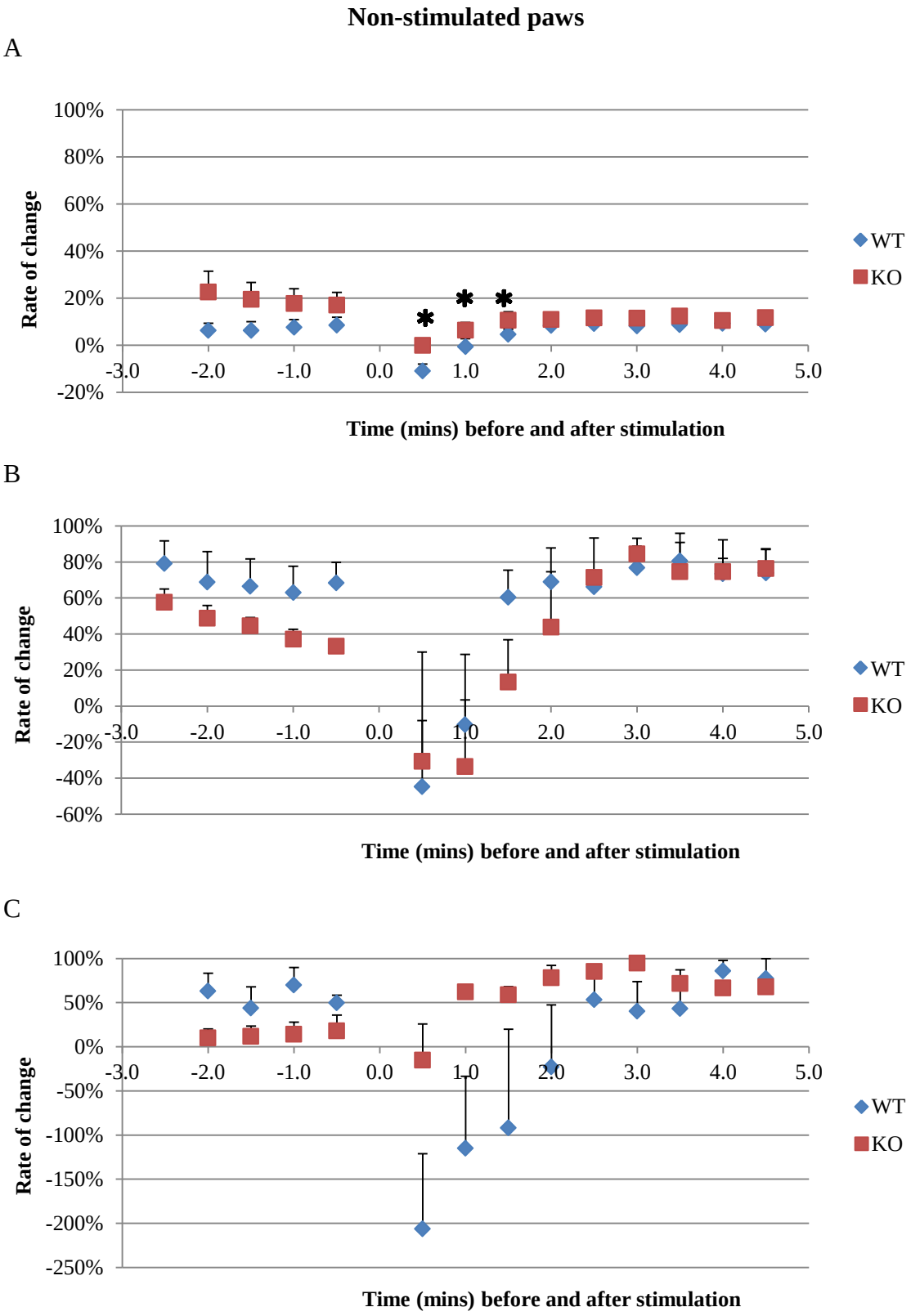
Non-stimulated paws
A
100%
80%
60%
40%
20%
0%
-20%
Rate of change
-3.0
-2.0
-1.0
0.0
1.0
2.0
3.0
4.0
5.0
Time (mins) before and after stimulation
WT
KO
B
100%
80%
60%
40%
20%
0%
-20%
-40%
-60%
Rate of change
Time (mins) before and after stimulation
WT
KO
C
100%
50%
0%
-50%
-100%
-150%
-200%
-250%
Rate of change
Time (mins) before and after stimulation
WT
KO

Figure 3.7. Average rate of change in non-stimulated hind paws

A. Average rate of change in total fluorescent counts in the non-stimulated paws before and after 100% xylene was applied topically (8 pairs).

B. B. Average rate of change in total fluorescent counts in the non-stimulated paws before and after 75% xylene was applied topically (3 pairs).

C. C. Average rate of change in total fluorescent counts in the non-stimulated paws before and after 5% formalin was injected (3 pairs).

The 0 marks the time for xylene application, error bars represent Standard Error of Mean (+SEM).

7. References

Bautista, W., McCrea, D. A., & Nagy, J. I. (2014). Connexin36 identified at morphologically mixed chemical/electrical synapses on trigeminal motoneurons and at primary afferent terminals on spinal cord neurons in adult mouse and rat. *Neuroscience*, *263*, 159–180. https://doi.org/10.1016/j.neuroscience.2013.12.057

Bautista, W., Nagy, J. I., Dai, Y., & McCrea, D. A. (2012). Requirement of neuronal connexin36 in pathways mediating presynaptic inhibition of primary afferents in functionally mature mouse spinal cord. *The Journal of Physiology*, *590*, 3821–3839. https://doi.org/10.1113/jphysiol.2011.225987

Bautista, W., Rash, J. E., Vanderpool, K. G., Yasumura, T., & Nagy, J. I. (2014). Re-evaluation of connexins associated with motoneurons in rodent spinal cord, sexually dimorphic motor nuclei and trigeminal motor nucleus. *European Journal of Neuroscience*, *39*(5), 757–770. https://doi.org/10.1111/ejn.12450

Bayliss, W. M. (1901). On the origin from the spinal cord of the vaso-dilator fibres of the hind limb, and on the nature of these fibres. *The Journal of Physiology*, *26*(3–4), 173–209. https://doi.org/10.1113/jphysiol.1901.sp000831

Bruce, N. A. (1913). Vaso-dilator axon-reflexes. *Quat. J. Exp. Physiol*, *6*, 339–354. https://doi.org/10.1113/expphysiol.1913.sp000144

Carmichael, N. M. E., Charlton, M. P., & Dostrovsky, J. O. (2009). Sex differences in inflammation evoked by noxious chemical, heat and electrical stimulation. *Brain Research*, *1276*, 103–111. https://doi.org/10.1016/j.brainres.2009.04.005

Carmichael, N. M. E., Dostrovsky, J. O., & Charlton, M. P. (2008). Enhanced vascular permeability in rat skin induced by sensory nerve stimulation: Evaluation of the time course

and appropriate stimulation parameters. *Neuroscience*, *153*(3), 832–841. https://doi.org/10.1016/j.neuroscience.2008.02.068

Caterina, M. J., Leffler, A., Malmberg, A. B., Martin, W. J., Trafton, J., Petersen-Zeitz, K. R., … Julius, D. (2000). Impaired nociception and pain sensation in mice lacking the capsaicin receptor. *Science*, *288*, 306–313.

Chapman, L. F., & Goodell, H. (1964). The participation of the nervous system in the inflammatory reaction. *Ann. N.Y. Acad. Sci.*, *116*(3), 990–1017.

Choi, C. M., & Bennett, R. G. (2003). Laser Dopplers to determine cutaneous blood flow. *Dermatologic Surgery*, *29*(3), 272–280. https://doi.org/10.1046/j.1524-4725.2003.29042.x

Clavelou, P., Pajot, J., Dallel, R., & Raboisson, P. (1989). Application of the formalin test to the study of orofacial pain in the rat. *Neuroscience Letters*, *103*(3), 349–353. https://doi.org/10.1016/0304-3940(89)90125-0

Cuello, A. C., Polak, J. M., & Pearse, A. G. E. (1976). Substance P: a Naturally Occurring Transmitter in Human Spinal Cord. *The Lancet*, *308*(7994), 1054–1056. https://doi.org/10.1016/S0140-6736(76)90968-5

Deans, M. R., Gibson, J. R., Sellitto, C., Connors, B. W., & Paul, D. L. (2001). Synchronous activity of inhibitory networks in neocortex requires electrical synapses containing connexin36. *Neuron*, *31*, 477–485. https://doi.org/10.1016/S0896-6273(01)00373-7

Dere, E., & Zlomuzica, A. (2012). The role of gap junctions in the brain in health and disease. *Neuroscience and Biobehavioral Reviews*, *36*(1), 206–217. https://doi.org/10.1016/j.neubiorev.2011.05.015

Dermietzel, R., & Spray, D. C. (2013). *Gap junctions, electric synapses*. *Neuroscience in the 21st Century: From Basic to Clinical*. https://doi.org/10.1007/978-1-4614-1997-6

Donnerer, J., Amann, R., & Lembeck, F. (1991). Neurogenic and non-neurogenic inflammation in the rat paw following chemical sympathectomy. *Neuroscience*, *45*(3), 761–765. https://doi.org/10.1016/0306-4522(91)90288-Y

Drygalski, A. von, Furla-Freguia, C., Mosnier, L. O., Yegneswaran, S., Ruf, W., & Griffin, J. H. (2012). Infrared fluorescence for vascular barrier breach in vivo- A novel method for quantitation of albumin efflux. *Thromb Haemost*, *108*(5), 981–991. https://doi.org/10.1160/TH12-03-0196.Infrared

Dubin, A. E., & Patapoutian, A. (2010). Nociceptors: The sensors of the pain pathway. *Journal of Clinical Investigation*, *120*(11), 3760–3772. https://doi.org/10.1172/JCI42843

Dubuisson, D., & Dennis, S. G. (1977). The formalin test: a quantitative study of the analgesic eefects of morphine, meperidine, and brain stem stimulation in rats and cats. *Pain*, *4*, 161–174.

Evans, W. H., & Martin, P. E. M. (2002). Gap junctions: structure and function (Review). *Molecular Membrane Biology*, *19*, 121–136. https://doi.org/10.1080/09687680210139

Flake, N. M., Hermanstyne, T. O., & Gold, M. S. (2006). Testosterone and estrogen have opposing actions on inflammation-induced plasma extravasation in the rat temporomandibular joint. *American Journal of Physiology. Regulatory, Integrative and Comparative Physiology*, *291*, R343–R348. https://doi.org/10.1152/ajpregu.00835.2005

Formaldehyde. (n.d.). Retrieved from https://en.wikipedia.org/wiki/Formaldehyde

Furshpan, E. J., & Potter, D. D. (1959). Transmission at the giant motor synapses of the crayfish. *J. Physiol.*, *145*, 289–325. https://doi.org/10.1113/jphysiol.1959.sp006143

Gamse, R., & Saria, A. (1987). Antidromic vasodilatation in the rat hindpaw measured by laser Doppler flowmetry: pharmacological modulation. *Journal of the Autonomic Nervous*

System, *19*(2), 105–111.

Gogan, P., Gueritaud, J. P., Horcholle-Bossavit, G., & Tyc-Dumont, S. (1977). Direct excitatory interactions between spinal motoneurons of the cat. *J. Physiol.*, *272*, 755–767.

Gonzalez, H. L., Carmichael, N., Dostrovsky, J. O., & Charlton, M. P. (2005). Evaluation of the time course of plasma extravasation in the skin by digital image analysis. *The Journal of Pain*, *6*(10), 681–688. https://doi.org/10.1016/j.jpain.2005.06.004

Green, P. G., & Levine, J. D. (2005). Sexual dimorphism in the effect of nonhabituating stress on neurogenic plasma extravasation. *European Journal of Neuroscience*, *21*, 486–492. https://doi.org/10.1111/j.1460-9568.2005.03872.x

Hartfield, E. M., Rinaldi, F., Glover, C. P., Wong, L.-F., Caldwell, M. A., & Uney, J. B. (2011). Connexin 36 expression regulates neuronal differentiation from neural progenitor cells. *PLoS ONE*, *6*(3), e14746. https://doi.org/10.1371/journal.pone.0014746

Helme, R. D., & McKernan, S. (1985). Neurogenic flare responses following topical application of capsaicin in humans. *Annals of Neurology*, *18*(4), 505–509. https://doi.org/10.1002/ana.410180414

Hinsey, J. C., & Gasser, H. S. (1930). The component of the dorsal root mediating vaso-dilatation and the sherrington contracture. *The American Journal of Physiology*, *92*(3), 679–689. https://doi.org/10.220.33.2

Hökfelt, T., Ljungdahl, A., Terenius, L., Elde, R., & Nilsson, G. (1977). Immunohistochemical analysis of peptide pathways possibly related to pain and analgesia: enkephalin and substance P. *Proceedings of the National Academy of Sciences of the United States of America*, *74*(7), 3081–3085. https://doi.org/10.1073/pnas.74.7.3081

Holton, P. (1959). Further observations on substance P in degenerating nerve. *J. Physiol.*, *149*,

35–36.

Holzer, P. (1988). Local effector functions of capsaicin-sensitive sensory nerve endings : Involvement of tachykinins, calcitonin gene-related peptide and other neuropeptides. *Neuroscience*, *24*(3), 739–768. https://doi.org/10.1016/0306-4522(88)90064-4

Holzer, P. (1998). Neurogenic vasodilatation and plasma leakage in the skin. *General Pharmacology*, *30*(1), 5–11. https://doi.org/10.1016/S0306-3623(97)00078-5

Jack, J. J. B. (1978). Some methods for selective activation of muscle afferent fibres. In *In Studies in Neurophysiology, Essays in Honor of Professor A.K. McIntyre (R. Porter, ed.)* (pp. 155–176). Cambridge University Press, Cambridge.

Jancso, G. (2009). *Neuroimmune biology. neurogenic inflammation in health and disease.* Amsterdam, Netherlands: Elsevier.

Jancso, N., Jancso-Gabor, A., & Szolcsanyi, J. (1967). Direct evidence for neurogenic inflammation and its prevention by denervation and by pretreatment with capsaicin. *Br. J. Pharmac. Chemother.*, *31*(1), 138–151. https://doi.org/10.1111/j.1476-5381.1967.tb01984.x

Langley, J. N. (1900). On axon -reflexes in the pre-ganglionic fibres of the sympathetic system. *The Journal of Physiology*, *25*(5), 364–398.

Lembeck, F. (1953). Zur Frage der zentralenÜbertragung afferenter Impulse—III. Mitteilung. Das Vorkommen und die Bedeutung der Substanz P in den dorsalen Wurzeln des Rückenmarks. *Arch. Exp. Path. Pharmak.*, *219*, 197–213.

Lembeck, F., & Holzer, P. (1979). Substance P as neurogenic mediator of antidromic vasodilation and neurogenic plasma extravasation. *Naunyn-Schmiedeberg's Archives of Pharmacology*, *310*, 175–183. https://doi.org/10.1007/BF00500282

Lemieux, M., Cabana, T., & Pflieger, J.-F. (2010). Distribution of the neuronal gap junction

protein connexin36 in the spinal cord enlargements of developing and adult opossums, Monodelphis Domestica. *Brain, Behavior and Evolution*, *75*, 23–32. https://doi.org/10.1159/000282173

Lewis, S. T. (1927). *The blood vessels of the human skin and their responses*. London, UK, Shaw and Sons.

Lewis, T., & Zotterman, Y. (1927). Vascular reactions of the skin to injury. Part VIII. The resistance of the human skin to constant currents, in relation to injury and vascular response. *J. Physiol.*, *62*(3), 280–288.

Li, C. L., & Bak, A. (1976). Excitability characteristics of the A- and C- fibers in a peripheral nerve. *Experimental Neurology*, *50*, 67–79.

Lisney, S. J. W., & Bharali, L. A. M. (1989). The axon reflex: An outdated idea or a valid hypothesis? *News in Physiological Sciences*, *4*(April), 45–48.

Lobanov, O. V., & Peng, Y. B. (2011). Differential contribution of electrically evoked dorsal root reflexes to peripheral vasodilatation and plasma extravasation. *Journal of Neuroinflammation*, *8*, 1–10. https://doi.org/10.1186/1742-2094-8-20

Logan, S. D., Pickering, A. E., Gibson, I. C., Nolan, M. F., & Spanswick, D. (1996). Electrotonic coupling between rat sympathetic preganglionic neurones in vitro. *Journal of Physiology*, *495*(2), 491–502.

Lynn, B., Geppetti, P., & Holzer, P. (1988). Neurogenic Inflammation. *Skin Pharmacol*, *1*, 217–224.

Maggi, C. A., Abelli, L., Giuliani, S., Santicioli, P., Geppett, P., Somma, V., … Meli, A. (1988). The contribution of sensory nerves to xylene-induced cystitis in rats. *Neuroscience*, *26*(2), 709–723.

McNamara, C. R., Mandel-Brehm, J., Bautista, D. M., Siemens, J., Deranian, K. L., Zhao, M., … Fanger, C. M. (2007). TRPA1 mediates formalin-induced pain. *Proceedings of the National Academy of Sciences of the United States of America*, *104*(33), 13525–13530. https://doi.org/10.1073/pnas.0705924104

Melzack, R., & Wall, P. D. (1999). *Textbook of pain*. Edinburgh New York Churchill Livingston.

Meyer, R. A., Raja, S. N., & Campbell, J. N. (1985). Coupling of action potential activity between unmyelinated fibers in the peripheral nerve of monkey. *Science*, *227*(4683), 184–187. https://doi.org/10.1126/science.3966152

Miampamba, M., Chery-Croze, S., Gorry, F., Berger, F., & Chayvialle, J.-A. (1994). Inflammation of the colonic wall-induced by formalin as a model of acute visceral pain. *Pain*, *57*, 327–334. https://doi.org/10.1016/0304-3959(94)90008-6

Nagy, J. I., Bautista, W., Blakley, B., & Rash, J. E. (2013). Morphologically mixed chemical-electrical synapses formed by primary afferents in rodent vestibular nuclei as revealed by immunofluorescence detection of connexin36 and vesicular glutamate transporter-1. *Neuroscience*, *252*, 468–488. https://doi.org/10.1016/j.neuroscience.2013.07.056

Pereda, A. E. (2014). Electrical synapses and their functional interactions with chemical synapses. *Nat Rev Neurosci*, *15*(4), 250–263. https://doi.org/10.1038/nrn3708

Pinter, E., & Szolcsanyi, J. (1995). Plasma extravasation in the skin and pelvic organs evoked by antidromic stimulation of the lumbosacral dorsal roots of the rat. *Neuroscience*, *68*(2), 603–614.

Pinter, E., & Szolcsanyi, J. (1996). Systemic anti-inflammatory effect induced by antidromic stimulation of the dorsal roots in the rat. *Neurosci Lett*, *212*, 33–36.

Pinter, E., Szolcsanyi, J., Pintér, E., & Szolcsányi, J. (1996). Systemic anti-inflammatory effect induced by antidromic stimulation of the dorsal roots in the rat. *Neurosci Lett*, *212*(1), 33–36. https://doi.org/10.1016/0304-3940(96)12766-X

Robertson, J. D., Bodenheimer, T. S., & Stage, D. E. (1963). The ultrastructure of Mauthner cell synapses and nodes in goldfish brains. *The Journal of Cell Biology*, *19*, 159–199.

Roveroni, R. C., Parada, C. A., Cecília, M., Veiga, F. A., & Tambeli, C. H. (2001). Development of a behavioral model of TMJ pain in rats: The TMJ formalin test. *Pain*, *94*(2), 185–191. https://doi.org/10.1016/S0304-3959(01)00357-8

Sándor, K., Helyes, Z., Elekes, K., & Szolcsányi, J. (2009). Involvement of capsaicin-sensitive afferents and the Transient Receptor Potential Vanilloid 1 Receptor in xylene-induced nocifensive behaviour and inflammation in the mouse. *Neuroscience Letters*, *451*(3), 204–207. https://doi.org/10.1016/j.neulet.2009.01.016

Szallasi, A., & Blumberg, P. M. (1999). Vanilloid (Capsaicin) receptors and mechanisms. *Pharmacological Reviews*, *51*(2), 159–212.

Szolcsányi, J. (1988). Antidromic vasodilatation and neurogenic inflammation. *Agents and Actions*, *23*, 4–11. https://doi.org/10.1007/BF01967170

Szolcsányi, J., Helyes, Z., Oroszi, G., Németh, J., Pintér, E., Szolcsányi J., … Pintér E. (1998). Release of somatostatin and its role in the mediation of the anti-inflammatory effect induced by antidromic stimulation of sensory fibres of rat sciatic nerve. *British Journal of Pharmacology*, *123*(5), 936–942. https://doi.org/10.1038/sj.bjp.0701685

Tjolsen, A., Berge, O.-G., Hunskaar, S., Rosland, J. H., & Hole, K. (1992). The formalin test: an evaluation of the method. *Pain*, *51*(1), 5–17. https://doi.org/10.1016/0304-3959(92)90003-T

Trevisani, M., Siemens, J., Materazzi, S., Bautista, D. M., Nassini, R., Campi, B., … Geppetti, P.

(2007). 4-Hydroxynonenal, an endogenous aldehyde, causes pain and neurogenic inflammation through activation of the irritant receptor TRPA1. *Proceedings of the National Academy of Sciences of the United States of America*, *104*(33), 13519–13524. https://doi.org/10.1073/pnas.0705923104

Wang, H.-L., & Lai, T. W. (2014). Optimization of Evans blue quantitation in limited rat tissue samples. *Scientific Reports*, *4*(6588), 1–7. https://doi.org/10.1038/srep06588

Watanabe, A. (1958). The interaction of electrical activity among neurons of lobster cardiac ganglion. *Jpn J Physiol.*, *8*(4), 305–318.

Wei, E. T., Kiang, J. G., Buchan, P., & Smith, T. W. (1986). Corticotropin-releasing factor inhibits neurogenic plasma extravasation in the rat paw. *The Journal of Pharmacology and Experimental Therapeutics*, *238*(3), 783–787.

Willis, W. D. (1980). *Spinal cord potentials. In: Windle WF, ed. The spinal cord: Its reaction to traumatic injury.* New York: Marcel Dekker Inc.

Yaprak, M. (2008). The axon reflex. *Neuroanatomy*, *7*, 17–19.

Yardeni, T., Eckhaus, M., Morris, H. D., Huizing, M., & Hoogstraten-Miller, S. (2011). Retro-orbital injections in mice. *Lab Animal*, *40*(5), 155–60. https://doi.org/10.1038/laban0511-155

Zhao, S. ting, Nagy, J. I., & Stecina, K. (2015). *Immunofluorescence study on the expression of Connexin 36 reporter eGFP and markers (Substance P, CGRP, TRPV1, TRPM8) in transgenic mice dorsal root ganglia nerves and its implication for the role of electrical coupling in mediating triple response*.